RANDOM-WALK MODELS FOR SIMULATING WATER VAPOR EXCHANGE

WITHIN AND ABOVE A SOYBEAN CANOPY

Bart J. J. M. van den Hurk
Agriculture University
Wageningen, The Netherlands

Dennis D. Baldocchi
Atmospheric Turbulence and Diffusion Division
Oak Ridge, Tennessee

NOTICE

Mention of a commercial company or product does not constitute an endorsement by NOAA/ERL. Use for publicity or advertising purpose, of information from this publication concerning proprietary products or the tests of such products, is not authorized.

ATDD Contribution File No. 90/5

CONTENTS

LIST OF TABLES

LIST OF FIGURES

LIST OF SYMBOLS

$'$	(prime) the time-fluctuating part of a quantity
$\overline{}$	(overbar) the time averaged part of a quantity
$''$	(double prime) the space-fluctuating part of a quantity
$<>$	(angled brackets) the space-averaged part of a quantity
a	coefficient in Markov sequence, $\exp(-\dfrac{\Delta t}{T_L})$
a_ℓ	leaf area density (m^2 m^{-3})
b	coefficient in Markov sequence, $\sqrt{1-\alpha^2}$
C_p	specific heat of air (J kg^{-1} K^{-1})
C_d	drag coefficient
c	scalar mixing ratio (g g^{-1})
c_i	scalar mixing ratio inside leaves (g g^{-1})
D	saturation vapor deficit of air (kPa)
d	zero plane displacement height (m)
E_c	evaporation flux density from a plant canopy (g m^{-2} s^{-1})
E_{eq}	equilibrium evaporation flux density (g m^{-2} s^{-1})
E_{imp}	imposed evaporation flux density (g m^{-2} s^{-1})
e	turbulent kinetic energy per unit mass (m^2 s^{-2})
e_a	water vapor pressure of air (kPa)
e_s	saturated water vapor pressure of air (kPa)
F	flux density (g m^{-2} s^{-1})
G	soil heat flux density (W m^{-2})
g	acceleration of gravity (m s^{-2})
g_c	canopy stomatal conductance (m s^{-1})
H	sensible heat flux density (W m^{-2})
h	canopy height (m)
K	turbulent diffusivity (m^2 s^{-1})
Kr	kurtosis
k	von Karman's constant (0.4)
L	Monin-Obukhov length scale (m)
ℓ	turbulence length scale
$P()$	joint probability density function
p	atmospheric pressure
Q	source strength per unit area (g m^{-2} s^{-1})
q	mass attributed to each particle (g)
R_n	net radiative flux density (W m^{-2})
Re	Reynold's number
r	vector location
r_b	laminar boundary layer resistance (s m^{-1})
r_n	random number
r_s	stomatal resistance (s m^{-1})
$S(z,t)$	diffusive source/sink strength of a layer of vegetation (g m^{-3} s^{-1})
s	change in saturated vapor pressure with temperature (kPa C^{-1})
T_L	Lagrangian time scale (s)

t	time (s)
T_a	time scale for acceleration of fluid parcels (s)
u	Eulerian longitudinal velocity (m s^{-1})
u*	friction velocity (m s^{-1})
V	volume (m^3)
v	Eulerian lateral velocity (m s^{-1})
w	Eulerian vertical velocity (m s^{-1})
W	Lagrangian vertical velocity (m s^{-1})
x	horizontal distance (m)
z	height (m)
z_o	roughness length (m)
α	coefficient in Langevin equation (T_L^{-1})
α_s	fraction of net radiation partitioned into conductive soil heat flux
β	coefficient in Langevin equation $\sigma_w\sqrt{2\alpha}$
e	$s\ \gamma^{-1}$
Δt	time step (s)
e_{tke}	dissipation rate of turbulent kinetic energy (m^2 s^{-3})
Γ	extinction coefficient for net radiation in a plant canopy
γ	psychrometric constant (K kPa^{-1})
γ_u	wind extinction coefficient
κ	molecular diffusivity of a scalar
λ	latent heat of evaporation (J g^{-1} K^{-1})
μ	mean random velocity (m s^{-1})
$\Omega(t)$	Gaussian white noise process
Ω_c	canopy evaporation coupling coefficient
ρ_a	air density (g m^{-3})
ρ_v	water vapor density (g m^{-3})
ρ_c	density of a scalar, c (g m^{-3})
σ_w	standard deviation in vertical velocity (m s^{-1})
σ_z	standard deviation in the vertical plume depth (m)

RANDOM-WALK MODELS FOR SIMULATING WATER VAPOR EXCHANGE WITHIN AND ABOVE A SOYBEAN CANOPY

Bart J.J.M. van den Hurk[1] and Dennis D. Baldocchi

ABSTRACT. The turbulent exchange of mass between a plant canopy and the atmosphere can be modelled with either Eulerian or Lagrangian models. The application of Eulerian models for estimating turbulent transfer within and above plant canopies has been criticized because of an inability to treat the dispersion of material from nearby sources well. Lagrangian models do not suffer from this deficiency since they consider the diffusion of material from both nearby and far away sources explicitly.

We developed three Lagrangian random walk models for computing the exchange of water vapor and water vapor mixing ratio profiles above and within a plant canopy. The movement of fluid parcels was computed using algorithms presented by Legg and Raupach (1982), Wilson et al. (1983) and Thomson (1984). The source strength of water vapor at discrete layers in the canopy was parameterized from estimates of net radiation flux density. The models were tested against measurement made within and above a soybean canopy.

Computed water vapor profiles, based on the algorithms of Legg and Raupach and Wilson et al., agree well with measured water values. However, subtle differences in the performance of these two models occurred. The model based on the Legg and Raupach formulation does a better job of predicting the water vapor concentration field inside the canopy while the model using the Wilson et al. algorithm yields more accurate computations of the mixing ratio profile above the canopy. The Lagrangian model based on the algorithm of Thomson computes water vapor profiles that severely underestimate measured values. The Thomson model is also incapable of computing a constant flux layer over the canopy after travel times of 100 s, as is possible with the other models. The Thomson model, though theoretically rigorous, suffers from limitations in its numerical formulation; small requisite time steps yield a negatively skewed third order moment in the random forcing term, which decreases the accuracy of generating a prescribed distribution of random numbers.

We also demonstrate that the validated Lagrangian models are more realistic in estimating water vapor mixing ratio profile inside a plant canopy than is an Eulerian model. The Eulerian model does not simulate the counter-gradient transfer of water vapor or the prominent 'nose' in the water vapor mixing ratio profile, which occurs because of the superposition of vapor from nearby sources on those from farther sources.

---

[1] Present address: Department of Meteorology, Agriculture University, Wageningen, The Netherlands

1

1. INTRODUCTION

An ability to accurately simulate turbulent fluxes and concentration profiles of passive and reactive scalars within and above plant canopies has many applications in the fields of meteorology, ecology, agriculture, atmospheric chemistry, biogeochemistry and plant physiology. For example, information on water vapor exchange is required to evaluate crop water use, as needed for irrigation scheduling, and hydrologic balances of watersheds. Information on CO_2 exchange is required to estimate the carbon balance of plant stands and ecosystems. Estimating the biogenic emission and deposition of reactive chemical species (i.e. methane, nitric oxide, ozone, and isoprene) is necessary for evaluating the chemical composition of the troposphere.

Two basic frames for modelling the turbulent transfer of gaseous compounds between a plant canopy and the atmosphere exist. They are the Eulerian and Lagrangian frames (see Meyers and Paw U, 1987; Raupach, 1988; Wilson, 1989). The Eulerian frame considers conservation processes at a fixed point in space, while the Lagrangian frame considers the transfer of fluid parcels as they are advected along the mean wind and diffuse. Below we present an overview of canopy turbulent transfer theory, to gain an appreciation of the strengths and weaknesses associated with the two frameworks. We then develop three Lagrangian random walk models for estimating water vapor profiles and fluxes. Finally, we test these models against measurements made in a soybean canopy.

2. Modeling Turbulent Transfer Within and Above Plant Canopies

2.1. Eulerian Turbulent Transfer Models

The Eulerian framework for modeling turbulent transfer starts with the conservation equation for a given scalar, which can be described by considering the processes that cause the mean mixing ratio of a scalar in a controlled volume to change. The mixing ratio of a scalar will change when the amount of material entering the volume does not equal that leaving. The rate of this change is dependent on the mean advective and turbulent flux divergences and the strength any sources or sinks that may occur therein. We are primarily interested in the simplified case of vertical turbulent transfer in a horizontally homogeneous layer. For this situation the conservation equation can be expressed as:

$$\frac{\partial \overline{<c>}}{\partial t} = -\frac{\partial \overline{<w'c'>}}{\partial z} + S(z,t) \tag{1}$$

where $<>$ denotes averaging in space, an overbar represents averaging in time and primes indicate departures from time-averaged values. t is time, z is height, w is vertical velocity. The covariance term, $\overline{w'c'}$, represents a turbulent flux in the vertical, F_z. $S(z,t)$ is the diffusive source-sink term attributed to the vegetation. It is defined as the amount of matter released or captured by a given volume per unit time. By invoking steady-state conditions, we can reduce Eq. 1 further to:

$$\frac{\partial \overline{<w'c'>}}{\partial z} = S(z) \tag{2}$$

The diffusive source/sink strength is typically parameterized with a resistance-analog relation (Finnigan, 1985; Meyers and Paw U, 1987):

$$S(z) = -\rho_a \, a_f(z) \, \frac{(c(z)-c(i))}{r_b(z)+r_s(z)}$$

(3)

where $a_f(z)$ is leaf area density, $c(z)$ is the scalar mixing ratio in the interstitial canopy air space, $c(i)$ is the scalar mixing ratio inside leaves, r_b is the laminar boundary layer resistance and r_s is the surface resistance, which primarily represents the resistance against diffusion through stomata.

To evaluate the variables c and r_b in Eq. 3 we must define the turbulence regime within the canopy. This is because the boundary layer resistance is a function of the local wind speed and the concentration gradient inside a plant canopy is a function of turbulent mixing. The budget equation for the wind velocity, after averaging in time and space, is given by (Raupach and Thom, 1981; Finnigan and Raupach, 1987; Meyers and Paw U, 1986; Raupach, 1988; Wilson, 1989):

$$\frac{\partial \langle u \rangle}{\partial t} = 0 = -\frac{\partial \langle u'w' \rangle}{\partial z} + f_F + f_V + f_B$$

(4)

u is horizontal wind velocity, f_F is the force against form drag, f_V the viscous drag force by plant elements on the mean flow and f_B is the buoyant force.

On inspection of the budget equations for mean scalar mixing ratios and wind velocity (Eqs. 1 and 4) one immediately observes that they contain additional unknown variables—higher order moments that represent the covariance between fluctuations in vertical velocity and the scalar being studied. Additional budget equations can be introduced to estimate these second order moments, but these additional budget equations include more unknowns—moments of the next higher order. We can only solve this system by obtaining an equal number of equations and unknowns, which must be done by parameterizing the higher order moments.

2.1.1 Parameterization of Turbulent Fluxes of Scalars Using First Order Closure or K-theory

Turbulent flux densities were initially described using K-theory, which assumes that the turbulent flux density of a scalar is analogous to molecular diffusion. In such circumstances the flux density is proportional to the local concentration gradient (see Raupach and Thom, 1981; Raupach, 1988):

$$\overline{w'c'} = -K \, \frac{\partial \bar{c}}{\partial z}$$

(5)

Although K-theory has been demonstrated to work well in the surface layer above plant canopies, its application inside plant canopies is limited. It can only be used with confidence if the length scales of turbulent transfer is less than the length scales associated with the curvature of the concentration gradient of the scalar. Furthermore, the turbulence length scale must not change over the distance where the concentration gradient changes significantly (Corrsin, 1974). Inside a canopy these assumptions are often not valid. Turbulent transfer is mainly associated with coherent gusts, whose length scales are comparable to or exceed the height of the crop. Over such distances the

concentration gradients usually changes significantly because wind speed profiles and the local sources vary markedly with height and have a profound influence on the concentration field. Experimental proof that K-theory can be invalid inside plant canopies comes from observations of counter-gradient transfer of mass and momentum (Denmead and Bradley, 1985; Baldocchi and Meyers, 1988a). Under such circumstances downward transport takes place against a negative concentration or wind velocity gradient. Counter-gradient flux occurs when strong concentration gradients are caused by "near-field" sources and the turbulent transfer of material is dominated by intermittent and large scale events (Raupach, 1987).

2.1.2 Second Order Closure Principles

Higher-order closure models have been proposed as a means of improving upon first order closure models (Meyers and Paw U, 1986, 1987; Wilson and Shaw, 1977; Wilson, 1989). These techniques include rate equations for the turbulent flux covariance and other arising second order moments, such as velocity variances. For instance, the budget equation for the vertical velocity-scalar density covariance is:

$$\frac{\partial \overline{<w'c'>}}{\partial t} = 0 = -\overline{<w'w'>}\frac{\partial \overline{<c>}}{\partial z} - \frac{\partial \overline{<w'w'c'>}}{\partial z} - \overline{<c'\frac{\partial p'}{\partial z}>} + g\frac{\overline{<\theta'c'>}}{\theta}$$

$$\qquad\qquad\qquad G \qquad\qquad T \qquad\quad P \qquad\quad B \qquad\qquad (6)$$

where g is the gravity acceleration, θ the potential temperature, and p is air pressure. The first term represents shear (gradient) production a of local turbulent flux, the second term represents transport, the third expression represents pressure interactions that destroys velocity-scalar correlations, and the fourth term represents the buoyancy production or sink.

Equations are also required to define the Reynold's stress and turbulent kinetic energy budgets. The Reynolds stress budget equation is:

$$\frac{\partial \overline{<w'u'>}}{\partial t} = 0 = -\overline{<w'w'>}\frac{\partial \overline{<u>}}{\partial z} - \frac{\partial \overline{<w'w'u'>}}{\partial z} - g\frac{\overline{<u'\theta'>}}{\theta} + \frac{\overline{<u'\partial p'>}}{\partial z} + \frac{\overline{<w'\partial p'>}}{\partial x} \qquad (7)$$

The terms on the RHS represent processes relating to gradient production, turbulent transport, buoyant production and velocity-pressure interactions.

Since the Reynolds stress equation contains velocity variance terms we must also define the turbulent kinetic energy (TKE) budget:

$$\frac{\partial \overline{<e>}}{\partial t} = 0 = -\overline{<u'w'>}\frac{\partial \overline{<u>}}{\partial z} - \frac{\partial \overline{<e'w'>}}{\partial z} + \rho_a\, C_p\, g\, \frac{\overline{<w'\theta'>}}{\theta} - \frac{\partial \overline{<w'p'>}}{\partial z} +$$

$$C_d\, a_f(z)\, (\overline{U^3} - \overline{u}\,\overline{uU}) - e_{tke} \qquad\qquad (8)$$

4

e is the TKE per unit mass ($e=\frac{1}{2}(\overline{w'w'}+\overline{u'u'}+\overline{v'v'})$), C_p is the specific heat of air, U is the wind speed, and ϵ_{tke} is the rate that TKE is dissipated as heat. The first term on the right hand is a shear production term. The second term defines the transport rate of TKE from one level to another. The third term represents buoyant production or loss. The fourth term represents pressure-velocity interactions, that drive the turbulence field towards isotropy. Work by velocity fluctuations against form drag is denoted by the fifth term.

Higher-order closure is generally achieved by invoking gradient diffusion arguments to parameter the highest-order moments (Wilson and Shaw, 1977; Meyers and Paw U, 1986, 1987; Wilson, 1989). The logic of attaining closure at higher orders was that any errors associated with parameterizing higher order terms would have little impact on estimates of lower moments, such as the flux covariance and its concentration field.

Deardorff (1978) is fundamentally critical of any closure approximations that rely on exchange coefficients and down-gradient diffusion. Deardorff argues that exchange coefficients are inadequate for near-field flows—which are predominant in the vicinity of sources and sinks. This is because a turbulent exchange coefficient in the vicinity of a source or sink is strongly related to the time period that fluid parcels have travelled. Most turbulence closure models use an exchange coefficient that represents the diffusion of material from far away. Deardorff (1978) correctly argues that the dispersion of a scalar released by a source at different times, or by sources at different distances upwind of an observer cannot be described by a single exchange coefficient.

The parameterization schemes of several other processes can also hamper higher order closure models. For example, inside a canopy work by the mean and turbulent flow against the canopy drag causes small-scale wakes in regions of the individual canopy elements. The energy of such small scale turbulent eddies is rapidly dissipated. Most closure models do not capture the physics of these processes well and tend to overestimate turbulent kinetic energy components inside the canopy (Meyers and Paw U, 1986). In spite of the theoretical weaknesses of closure models we must admit that validation tests in plant canopies have been reasonably successful (Meyers and Paw U, 1986; 1987).

2.2 The Lagrangian Framework

In the Lagrangian framework a concentration field is related to the statistics of an ensemble of dispersing marked fluid parcels. The Lagrangian approach is valid if the turbulent diffusion of the fluid parcel far exceeds the molecular diffusion of scalar material confined within the parcel. Below we give a brief review on the subject. Additional reviews are presented by Lamb (1980), Sawford (1985), Raupach (1988) and Wilson (1989).

From first principles, a concentration is simply defined as the number of fluid parcels (n) observed in a given volume (V) at a specified vector location (r) and time (t):

$$c(r,t)=\frac{n(r,t)}{V} \qquad (9)$$

To evaluate Eq. 9 we must introduce a joint probability density function, $P(r,t \mid r_o,t_o)$, to define the probability that a fluid parcel released from a point in space (r_o) and time (t_o) will be observed at another location and time (r,t):

The conditional probability of a fluid parcel, labelled X_n, equals one if it is released from a reference location (z_o) at an initial time (t_o) and arrives at a volume centered on location z at time t; otherwise X_n is zero. This probability density function depends only on the properties of the turbulent wind field.

$$P(r,t \mid r_o,t_o) - \lim_{N \to \infty} (\frac{1}{N}) \sum_{n-1}^{N} X_n dV \qquad (10)$$

In the natural environment we may have many sources. The ensemble mean concentration at a point and time is then defined by superposing the probabilities that fluid parcels that had been released from upwind sources will arrive, through turbulent diffusion and transport, at a specified receptor under a given time interval. If we consider a plant canopy that is horizontally homogeneous then turbulent transfer varies only in the vertical direction (z). Under this condition the ensemble mean concentration is defined by integrating over space the product of the source/sink strength at the origin and the joint probability density function for fluid motion:

$$c(z,t) - \int_0^t \int_0^z P(z,t \mid z_o,t_o) \, S(z_o,t_o) dz_o \, dt_o \qquad (11)$$

2.2.1 Turbulent Diffusion in a Homogeneous Field

The ultimate goal of our work is to develop a model for evaluating turbulent diffusion in plant canopy, where the turbulent field varies in space and the turbulent statistics do not have a Gaussian distribution. To gain a full understanding of Lagrangian turbulent diffusion it is instructive to first consider diffusion under ideal conditions, where turbulent statistics are distributed in a Gaussian manner and the turbulent field is invariant in space (it is homogeneous).

The classic description of turbulent motion in homogeneous turbulence is attributed to Taylor (1921). Below we give a brief description of his analysis. For simplicity we will only consider vertical diffusion since it is most applicable to our examination of diffusion in and above a plant canopy. From first principles, the position of a fluid parcel is defined by integrating its velocity over a given time interval:

$$Z(t) - \int_0^t W(t') dt' \qquad (12)$$

6

In analyzing turbulence we generally evaluate mean quantities. However, the mean position is of no interest here because the mean vertical velocity is zero in homogeneous turbulence. Hence, its mean position is equal to the origin. Instead the spread of the plume is of greater interest. The trick to evaluating its spread is to multiply Eq. 12 by the vertical velocity, W(t). This operation yields:

$$W(t)Z(t) - \frac{dZ(t)}{dt}Z(t) - \frac{d\frac{1}{2}Z(t)^2}{dt} - \int_0^t W(t)W(t')dt' \qquad (13)$$

If we average Eq. 13, we arrive at an equation describing the time rate of change of the plume variance:

$$\frac{d\overline{Z(t)^2}}{dt} - 2\int_0^t \overline{W(t)W(t')}dt' - 2\overline{W^2}\int_0^t R_W(\tau)d\tau \qquad (14)$$

Eq. 14 contains a covariance term, $\overline{W(t)W(t')}$, that needs further explanation. This term represents the correlation between velocities at different times, t and t', which can be expressed in terms of an autocorrelation function, $R_W(\tau)$. Eq. 14 takes on different expressions if it is solved at two limits, after a short and a long travel time.

Near field diffusion refers to the case when the travel time is much less than the Lagrangian turbulence time scale (T_L). In this regime fluid parcel motion is highly persistent, so the vertical velocity autocorrelation coefficient equals one. Consequently, the integration of Eq. 14 with respect to time yields:

$$\overline{Z^2} - \overline{W^2}t^2 \qquad (15)$$

The interpretation of Eq. 15 is that the diffusion of a plume close to a source is linearly dependent on travel time.

Far field diffusion refers to the case where travel time exceeds the turbulence time scale. Parcel motion in the far field is not correlated with initial conditions and can be assumed random. The integration of the autocorrelation function approaches the value of the Lagrangian turbulence time scale, T_L, as the integration interval approaches infinity:

$$T_L - \frac{1}{\overline{W'W'(0)}} \int_0^\bullet \overline{W'(0)W'(t)}dt \qquad (16)$$

Inserting this identity into Eq. 14 and solving for the differential equation yields:

$$Z^2 - \overline{W^2}\ t\ T_L \qquad t > T_L \qquad (17)$$

7

Far field diffusion produces a plume whose standard deviation grows in proportion to the square root of travel time.

2.2.2 Formulations of Diffusion Models Based on the Langevin Equation.

A model for turbulent diffusion can be based on the Langevin equation. The Langevin equation was originally used as a theory to describe Brownian motion. In the last decade, the Langevin Equation has been used often to describe turbulent dispersion in the atmospheric boundary layer and in model and real plant canopies (Hall, 1975; Reid, 1979; Hunt and Weber, 1979; Durbin, 1980; Wilson et al., 1981a, 1981b, 1981c, 1983; Legg and Raupach, 1982; Legg, 1983; Thomson, 1984; Sawford, 1985; Walklate, 1987; Leclerc et al., 1988; Aylor, 1989 among others).

The Langevin equation is a stochastic differential equation for the acceleration or time rate of change of a velocity component. For vertical velocity (W) it is given by:

$$\frac{dW}{dt} = -\alpha \; W + \beta \; \Omega(t) \tag{18}$$

where α and β are coefficients that are defined below. $\Omega(t)$ is a Gaussian "white noise" process. The Langevin Equation defines the acceleration of a fluid parcel (dw/dt) as a function of the memory of its current value and a random forcing. The random forcing function $\Omega(t)$ is defined such that no two subsequent events are correlated. It has a mean of zero and a variance of one. The Langevin Equation cannot be rigorously derived from the Navier-Stokes equation for fluid motion. Use of the Langevin equation to simulate Markovian particle movement is justified by its ability to resemble many properties that are observed in homogeneous turbulence (Sawford, 1985).

The Langevin Equation can be solved analytically. For completeness we give the solution shown by Legg and Raupach (1982):

$$W(t) = W(0)\exp(-\alpha t) + \beta \int_0^t \exp(\alpha(t_s - t))\Omega(t_s)dt_s \tag{19}$$

where W(t) is considered to be a function of its initial value (W(0)) and a random term. Averaging the terms in Eq. (19) yields for the mean vertical velocity:

$$\overline{W(t)} = \overline{W(0)}\exp(-\alpha t) \tag{20}$$

The second term in Eq. 17 vanishes since $\overline{\Omega(t_s)} = 0$. Fluctuations about the mean (') are given by:

$$W'(t) = W'(0)\exp(-\alpha t) + \beta \int_0^t \exp(\alpha(t_s - t))\Omega(t_s)dt_s \tag{21}$$

An important measure for the determination of the spreading of motion (ie. the spreading of a cloud) is the variance of the vertical motion around its mean value. This variance can be derived from Eq. 21 by taking the mean value of the W' squared:

$$\overline{W'W'(t)} = \overline{W'W'(0)}\exp(-2\alpha t) + \beta^2 \int_0^t \int_0^t \exp(\alpha(t_s - t))\exp(\alpha(t_u - t))\overline{\Omega(t_s)\Omega(t_u)}dt_s dt_u \qquad (22)$$

Because no correlation exists between $\Omega(t_s)$ and $\Omega(t^u)$, this equation can be simplified to:

$$\overline{W'W'(t)} = \overline{W'W'(0)}\exp(-2\alpha t) + \beta^2 \int_0^t \exp(2\alpha(t_s - t))dt_s \qquad (23)$$

Evaluating the integral yields:

$$\overline{W'W'(t)} = \overline{W'W'(0)}\exp(-2\alpha t) + \frac{\beta^2}{2\alpha}(1 - \exp(-2\alpha t)) \qquad (24)$$

The coefficients α and β can be derived by considering the covariance for w between time 0 and t:

$$\overline{W'(0)W'(t)} = \overline{W'W'(0)}\exp(-\alpha t) \qquad (25)$$

The coefficient α in Eq. 25 must be a function of the time scale of the motion, since the correlation of w between time 0 and time t decreases as the time proceeds. From Eqs 24 and 25 α is defined as:

$$\alpha = \frac{1}{T_L} \qquad (26)$$

If the mean vertical velocity equals zero then:

$$\beta = \sigma_w\sqrt{2\alpha} = \sigma_w\sqrt{\frac{2}{T_L}} \qquad (27)$$

where σ_w is the Lagrangian velocity variance. For simplicity, it is assumed that the Lagrangian and Eulerian velocity variances are identical.

2.2.3 Derivation of the Markov-process equation for vertical velocity

Inside a plant canopy mean wind velocity and its statistics vary appreciably with height and are non-Gaussian (Wilson et al., 1982; Baldocchi and Meyers, 1988a, 1988b; Raupach, 1988). The joint probability density function, P(), cannot be specified analytically in non-Gaussian, inhomogeneous turbulence. Yet, it can be determined numerically by assuming that the turbulent diffusion is Markovian and by assuming that the motion of an ensemble of fluid parcels can be described with

9

the Langevin Equation. A Markov process is a stochastic process that is formulated on the following principle:

> "if the state of a system at a particular time is known, additional information regarding the behavior of the system at times in the past have no effect on our knowledge of the probable development of the system in the future" (Arnold, 1974).

Markov processes are continuous, but are not differentiable (Legg and Raupach, 1982). At first glance, this restraint would restrict the use of a Markov model to represent turbulent flow—models of turbulent flow must be differentiable, otherwise infinite accelerations will occur. This restriction is not insurmountable if we examine the Markov sequence of fluid parcels velocities at discrete time steps instead of evaluating the system as a continuous Markov process. Application of a Markov sequence is based on the restriction that the difference between time steps (Δt) must exceed that of a time scale defining the period over which fluid parcel accelerations are correlated ($t_k = Re^{0.5} T_L$, Re is Reynolds number and T_L is the Lagrangian integral time scale).

The vertical velocity of a particle at time t is determined by its speed at time of the past time step (t-Δt) and a random contribution to its movement. The Markov sequence is given by:

$$W_{n+1} = aW_n + b\sigma_W r_n \tag{28}$$

where r_n is a Gaussian random number with zero mean and unit variance. The coefficients a and b are given by (Legg and Raupach, 1982):

$$a = \exp(-\alpha \Delta t) = \exp(-\frac{\Delta t}{T_L}) \tag{29}$$

and

$$\sigma_W^2 b^2 = \frac{\beta^2}{2\alpha}(1 - \exp(-2\alpha \Delta t)) = \sigma_W^2(1 - a^2) \tag{30}$$

and hence,

$$b = \sqrt{1 - a^2} \tag{31}$$

The time step Δt must be much greater than T_a, the acceleration time scale; T_a is in order of $T_L Re^{-1/2}$ (Tennekes and Lumley, 1972). On the other hand, the period between time steps must be small in inhomogeneous turbulence to keep the fractional change in T_L small between time steps. Δt cannot exceed the Lagrangian time scale T_L without losing essential information about the motion (Sawford, 1984). Thus $T_a << \Delta t << T_L$.

2.2.4 Adapting the Markov Random Walk Model for Varying Velocity Statistics

Until now, we have not theoretically considered the variation of σ_w^2 with height. The vertical gradient in the vertical velocity variance mathematically imposes a downward drift on the Markovian random walk model. The net downward drift is caused by the arrival of downward directed fluid parcels from above into a lower region with a decreased vertical velocity scale and a reduced probability of leaving that region (Raupach, 1988; Sawford, 1985). Accumulation of matter under a plant canopy does not occur in such circumstances because intermittent gusts disproportionately transport matter and maintain continuity. Heuristic attempts have been made to remove the unrealistic accumulation of matter in a field of inhomogeneous turbulence. One approach introduces an additional force term into the Langevin equation, which translates into a mean upward drift velocity in the solution of the differential equation (Wilson et al., 1981a, 1981b; Legg and Raupach, 1982; Thomson, 1984). Below we describe the random walk algorithms of Legg and Raupach, Wilson and colleagues, and Thomson. These algorithms will later be adapted to simulate water vapor transfer in a soybean canopy.

a) Legg and Raupach Model

Legg and Raupach (1982) argued that the variation of σ_w^2 with height must be related to the mean vertical pressure gradients due to the incompressibility of air:

$$\frac{\partial \sigma_w^2}{\partial z} - -\frac{1}{\rho}\frac{\partial \overline{p}}{\partial z} \qquad (32)$$

where p is the mean air pressure at height z. $\partial p/\partial z$ acts against the downward drift. The Markov sequence model can be re-derived from a modified Langevin Equation that takes into account the additional force due to the balance between the vertical gradient in the vertical velocity variance and the pressure gradient:

$$\frac{dW}{dt} - -\alpha W + \beta \Omega(t) + \frac{\partial \sigma_w^2}{\partial z} \qquad (33)$$

The solution of Eq. 33 is:

$$W(t) - W(0)\exp(-\alpha t) + \beta \int_0^t \exp(\alpha(s-t))\Omega(s)ds + \frac{\partial \sigma_w^2}{\partial z}\alpha^{-1}(1-\exp(-\alpha t)) \qquad (34)$$

The mean vertical velocity is given by:

$$\overline{W(t)} = \overline{W(0)}\exp(-\alpha t) + \frac{\partial \sigma_w^2}{\partial z}\alpha^{-1}(1-\exp(-\alpha t)) \tag{35}$$

When $\overline{W(t)} = \overline{W(0)}$, Eq. 35 reduces to

$$\overline{W(t)} \equiv \frac{\partial \sigma_w^2}{\partial z}T_L \tag{36}$$

The Markov sequence is:

$$W_{n+1} = aW_n + b\sigma_W r_{n+1} + c \tag{37}$$

The definitions of a and b are unchanged. c is given by:

$$c = \frac{\partial \sigma_w^2}{\partial z}T_L(1-\exp(\frac{\Delta t}{T_L})) \tag{38}$$

b) <u>The model of Wilson and colleagues.</u>

Wilson et al., (1981a, 1981b, 1983) developed a Markov sequence particle trajectory method for inhomogeneous turbulence that employs a transformed coordinate system. The purpose of the transformation is to allow vertical motions to have equal time scales at all heights (as in homogeneous turbulence). The random-walk Markov model for inhomogeneous turbulence (they denote as WTK" is:

$$\frac{W_{n+1}}{\sigma_{W\,n+1}} = a\frac{W_n}{\sigma_{W\,n}} + br_{n+1} + \gamma T_L\frac{d\sigma_W}{dz} \tag{39}$$

where $\qquad \sigma_{W\,n+1} = \sigma_{W\,n} + W_n\Delta t\dfrac{d\sigma_W}{dz}$ and $\gamma = (1-a)$.

c) <u>Thomson (1984) model.</u>

Thomson (1984) defined the Markov sequence model as:

$$W_{n+1} = \alpha W_n + \mu_{n+1} \tag{40}$$

where μ is a random velocity. Thomson's approach is attractive because he defined the higher moments of the random term in the Markov sequence using moment generating functions to account for non-Gaussian and inhomogeneous turbulence which occurs in plant canopies. The first three moments (mean, variance, and skewness) of the random vertical velocity term are:

$$\overline{\mu_{n+1}} - \Delta t \frac{\partial \overline{W'W'}}{\partial z} + O(\Delta t^2) \tag{41}$$

$$\overline{\mu_{n+1}^2} - \Delta t \frac{\partial \overline{W'W'W'}}{\partial z} + 2 \frac{\Delta t}{T_L} \overline{W'W'} + O(\Delta t^2) \tag{42}$$

$$\overline{\mu_{n+1}^3} - \Delta t \frac{\partial \overline{W'W'W'W'}}{\partial z} + 3 \frac{\Delta t}{T_L} \overline{W'W'W'} - 3 \Delta t \overline{W'W'} \frac{\partial \overline{W'W'}}{\partial z} + O(\Delta t^2) \tag{43}$$

The symbol O denotes an error term which has the order of magnitude of Δt^2. Note that the second order moment contains a third order moment term, $\overline{w'w'w'}$ and the third moment has a fourth moment term.

3. ADAPTING A LAGRANGIAN RANDOM-WALK MODEL FOR COMPUTING WATER VAPOR CONCENTRATION AND FLUX PROFILES ABOVE AND WITHIN A UNIFORM SOYBEAN CANOPY

3.1 Random Number Generation and Distributions

Markov sequence models are linked to a random component. This component has a distribution, described by a mean, variance, skewness, and kurtosis, that must be accurately generated via numerical techniques. Random numbers were computed with the rejection technique (Spanier and Gelbard, 1969). The technique involves selecting two random numbers in the interval between 0 and 1. The first random number (RE1) is used to compute a transformed variable (y) that has a mean of zero and a variance of one:

$$y - \frac{(RE1 - \overline{x})}{\sigma_x} \tag{44}$$

The transformed variable is then used to compute the value of the probability density function (p(y)). The second random number, RE2, is compared against p(y). If RE2 is less than p(y) then it is accepted as the random number. Otherwise, two more random numbers are selected and the exercise is repeated.

The Gram-Charlier distribution was used to compute the probability density function (p(y))

$$p(y) = \frac{1}{\sigma_y \sqrt{2\pi}} \exp(-\frac{y^2}{2}) [1 + \frac{Sk}{6}(y^3 - 3y) + \frac{(Kr-3)}{24}(y^4 - 6y^2 + 3)] \qquad (45)$$

The Gram-Charlier distribution is capable of computing normal and non-normal random number distributions. For example, when skewness (Sk) is zero and kurtosis (Kr) is three the Gram-Charlier distribution is reduced to a Gaussian probability density function.

Figure 3.1 shows the probability distributions of random numbers computed for a Gaussian and skewed distribution. The distribution of random numbers are compared against values computed analytically with the Gram-Charlier distribution. The prescribed Gaussian distribution has a mean of zero and a variance of 1. The random number algorithm, described above, computed a set of numbers that approached the prescribed values; the mean was 0.000 and the variance was 0.972. The skewed case prescribed a mean of zero, variance of one, and skewness of -2.122. Here, we simulated a distribution with a mean of 0.044 and a variance of 0.975. Below we discuss the consequences of the inability to compute a skewed random number distribution with a perfect zero mean.

3.2 Computation of the Vertical Source Distribution

The Markov sequence models, described above, tell where a fluid parcel will probably go. To use these formulations to calculate the concentrations and the transfer of water vapor within and above a plant canopy we must also assess the source strength of water vapor at different layers in a plant canopy. The diffusive source density, S, is defined as the amount of matter released from a given volume per unit of time. Its units are g m^{-3} s^{-1}. The source density at height z, in a horizontally homogeneous canopy, is computed s the divergence of the scalar flux density (F) at that height:

$$S(z) = \frac{\partial F}{\partial z} \qquad (46)$$

Evaporation from the soil can also contribute to the water vapor concentration profile inside a plant canopy (Denmead, 1964). By integrating the source density, with respect to height, we can arrive at the total source strength per unit surface area (Q) from an evaporating plant canopy:

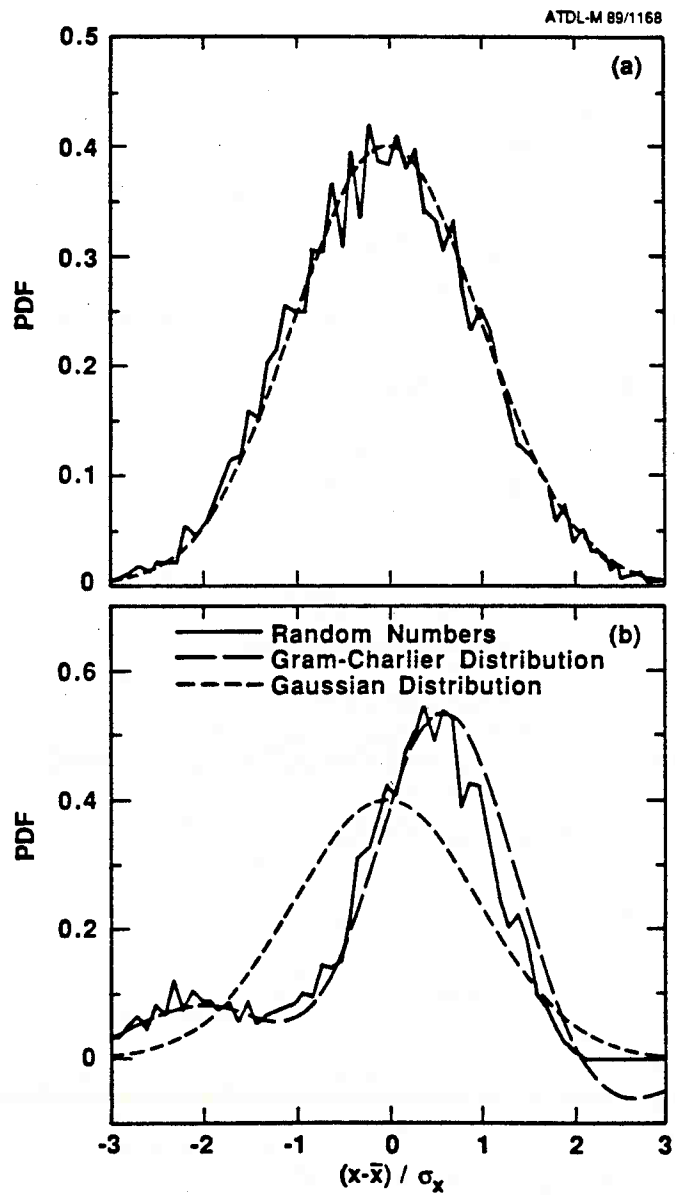$$Q = \int_0^h S(z)\,dz + E_s \qquad (47)$$

Fig. 3.1

Comparison between the probability distribution of random numbers computed with the rejection technique and the analytical model.

Evaporation from a plant canopy (E_c) proceeds at a rate somewhere between the value of equilibrium evaporation (E_{eq})—which is a function of the net radiation balance—and the imposed evaporation E_{imp}, which is a function of the stomatal conductance and the vapor pressure deficit (Jarvis and McNaughton, 1986):

$$E_c - \Omega_c E_{eq} + (1 - \Omega_c) E_{imp} \qquad (48)$$

Ω_c is a measure of the coupling between conditions at the canopy surface and the free airstream. Ω_c is a function of temperature, boundary layer resistance, and stomatal resistance (Jarvis and McNaughton, 1986). Ω ranges between 0 and 1. Low values are associated with strongly coupled canopies, such as tall, aerodynamically-rough forests that are exposed to high winds. Values approaching one are associated with short, aerodynamically-smooth crops, such as alfalfa and soybeans (Jarvis and McNaughton, 1986), that are weakly coupled to their overhead environment.

The equilibrium evaporation can be defined by examining the time rate of change of humidity in a well-mixed control volume, or box. The time rate of change of humidity in a controlled volume will be proportional to the rate of the water vapor flux into the box. Eventually an equilibrium flux density will be met between the vapor pressure deficit driving the gradient flux and the energy input into the system to evaporate water. This yields a relationship of evaporation defined as:

$$\lambda E_{eq} - \frac{s}{s + \gamma} (R_n - G) \qquad (49)$$

λ being the latent heat of evaporation, R_n is the net radiation at z in the canopy, G the soil heat flux (G is neglected for the individual layers inside a canopy), s is the rate of change of saturated vapor pressure with changing temperature), and γ is the psychrometric constant.

The imposed evaporation, on the other hand, is proportional to the product of the canopy stomatal conductance and the saturation vapor deficit (D):

$$E_{imp} - \frac{g_c D}{P} \qquad (50)$$

P is atmospheric pressure and g_c is the conductance to water vapor transfer.

The evaporative flux density of short, well-watered, vegetated surfaces, like soybean canopies, is strongly coupled to the amount of available energy (Jarvis and McNaughton, 1986). We, therefore, assumed that its evaporative source strength is a function of the equilibrium evaporation rate:

$$E(z) - 1.3 \frac{s}{\lambda(s + \gamma)} R_n(z) \qquad (51)$$

16

The coefficient 1.3, in Equation 51, is a value commonly reported in studies measuring the ratio between E_c and E_{eq} (Priestly and Taylor, 1972; Brutsaert, 1982).

An estimate of the net radiation flux density inside a canopy is needed to evaluate Eq. 51. We computed R_n according to Beer's law of extinction of radiation (Monteith, 1973):

$$R_n(z) - R_n(h)\exp(-\Gamma \int_z^h a_l(z)dz))$$ (52)

where $R_n(h)$ is the net radiation flux density at the top of the canopy, $a_l(z)$ is leaf area density and Γ is an extinction coefficient. The integral of $a_l(z)$ with respect to z represents cumulative leaf area per unit ground area.

3.3 Computation of Concentration and Vertical Flux

The canopy was divided into 10 layers for computations of the water vapor source profile. Fluid parcels were released from each level in proportion to its source strength. An initial vertical velocity was given to each marked parcel, using $\sigma_w(z)\, r_1$. The vertical velocity of each particle is computed at successive time steps using one of the Markov sequence models described above. The altitude of at each time step, i, was computed by:

$$z_{i+1} - z_i + w_i \Delta t$$ (53)

The domain in which parcel traveled contained 40 equally spaced layers and extended up to 4 times canopy height. Fluid parcels intercepting the soil surface were perfectly reflected upward. Since canopy turbulence is inhomogeneous, new values of the turbulence statistics (σ_w, σ_w^2, σ_w^3 and T_L) were evaluated at each time step to compute a new vertical velocity, w_{i+1}.

Concentrations are equal to the ratio between the mean horizontal flux of water vapor and the mean wind velocity (Raupach, 1989). The horizontal flux is proportional to the total streamwise distance traveled by the parcels within a given vertical layer as a fluid parcel travels for a given time interval. The following algorithm was used to compute concentrations from the random walk simulations:

$$\bar{c}(z,t) - \frac{q_{part}\sum_{i-1}^{N}\sum_{j-1}^{t} \Delta t_{i,j} U(z)_{i,j}}{\Delta z\ \overline{U(z)}}$$ (54)

q_{part} is the mass attributed to each parcel. Δz is the vertical thickness of each layer. The total concentration profile is determined by the superpositioning the releases from all the water vapor sources in the canopy. The normalized vertical flux, $\dfrac{\overline{w'c'}}{Q}$, is defined as the ratio between the net number of fluid parcels that cross a horizontal plane at height z and the total number of fluid parcels that were released (Raupach, 1989).

Contributions from the soil are added to those from the lowest layer, as recommended by Raupach (1989). We assumed that soil evaporation proceeds at a rate proportional to the amount of energy available at the soil. E_s is computed as:

$$E_s = 1.3 \frac{s}{\lambda(s+\gamma)}(R_n(0)-G) \tag{55}$$

Soil heat flux is estimated as a function of net radiation at the soil:

$$G = \alpha_s R_n \tag{56}$$

where α_s is an empirical constant, on the order of 0.5 (Choudhury et al., 1987).

3.4 Turbulence Statistics

The horizontal windspeed (u) was computed as a function of altitude, z. No fluctuations of the horizontal velocity were considered. Inside the canopy the horizontal wind speed was computed as an exponential function of canopy height (h) (Cionco, 1972):

$$\overline{u(z)} = \overline{u(h)} \exp(\gamma_u(\frac{z}{h}-1)) \tag{57}$$

where γ_u is an extinction-coefficient that depends on the canopy density and structure. Its value for agricultural crops is usually between 1.5 and 2.8 (Raupach and Thom, 1981). Above the canopy a logarithmic profile was used to compute wind speed:

$$\overline{u(z)} = \frac{k}{u_*}\ln(\frac{z-d}{z_o}) \tag{58}$$

where u* is the friction velocity, k the Karman constant (assumed to be 0.4), d is the displacement height and z_o the roughness length. Both d and z_o are assumed to be proportional to the crop height. The values of u(h), the wind attenuation coefficient (γ), the displacement height and roughness length are given in Table 3.1.

Table 3.1 Canopy properties of the soybean Clark cv. on August 4, 1979.

parameter	symbol	value
crop height	h	0.85 m
roughness length	z_0	0.073 h
zero plane displacement	d	0.6 h
net radiation extinction coeff.	Γ	0.55
leaf area index	LAI	4.1

The standard deviation in vertical velocity (σ_w) was parameterized as being linear inside the canopy from 0.125 u* at z = 0 to 1.25 u* at z = h (Hunt and Weber, 1979). Above the canopy σ_w was assumed constant with height. These values agree very well with observations in a corn canopy (Wilson et al., 1982). The value of T_L was computed with the formulation of Raupach (1989). T_L was regarded as constant in the canopy and equal to 0.3 h/u*. Above this height T_L was computed as $T_L(z) = T_L(h)^{0.5}$.

Skewness is a measure of the probability of "extreme events". Skewness of the vertical wind velocity component is typically negative inside canopies (indicative of occasional downward gusts), but decreases with decreasing canopy height and structure complexity. Baldocchi and Meyers (1988b) measured skewness of the three wind velocity components in a deciduous forest, while Baldocchi and Hutchison (1987) observed turbulence skewness inside an almond orchard. Typical values for the latter canopy of Sk_w were about -0.3. In a windtunnel study Raupach et al. (1986) observed a negative skewness of the vertical velocity component ranging from 0 (z=h), decreasing to about -0.7 (z/h = 0.5), and increasing to zero again when the surface was reached. Raupach (1988) parameterized the inside canopy skewness of w as a constant value for z ≤ h (ranging between -0.5 and -1.0), and decreasing to zero at z = 1.5h. In this study will Sk_w be parameterized in this way. Skewness effects are only considered in the model of Thomson (1984).

3.5 Experimental Details and Measurements of Canopy Structure

Measurements of latent energy flux densities and water vapor profiles above and within a soybean (Glycine max L. Merrill) canopy were used to test the random walk models. These data are reported in Baldocchi (1982). The meteorological variables were measured above and within a Clark cultivar near Mead, NE. We used data acquired on August 4, 1979, between 11 am and 2 pm. The field size was 105 x 219 m. The plants were planted in 0.75 m wide rows that ran north to south. During the measurement period the wind blew down the rows. The fields were irrigated and the water status of the crop was considered to be well watered.

Fig. 3.2 gives the profiles of leaf area density, $a_\ell(z)$, and cumulative leaf area index. The leaf area density data was fit to a Beta distribution (see Meyers and Paw U, 1986), to get a continuous curve for modelling purposes.
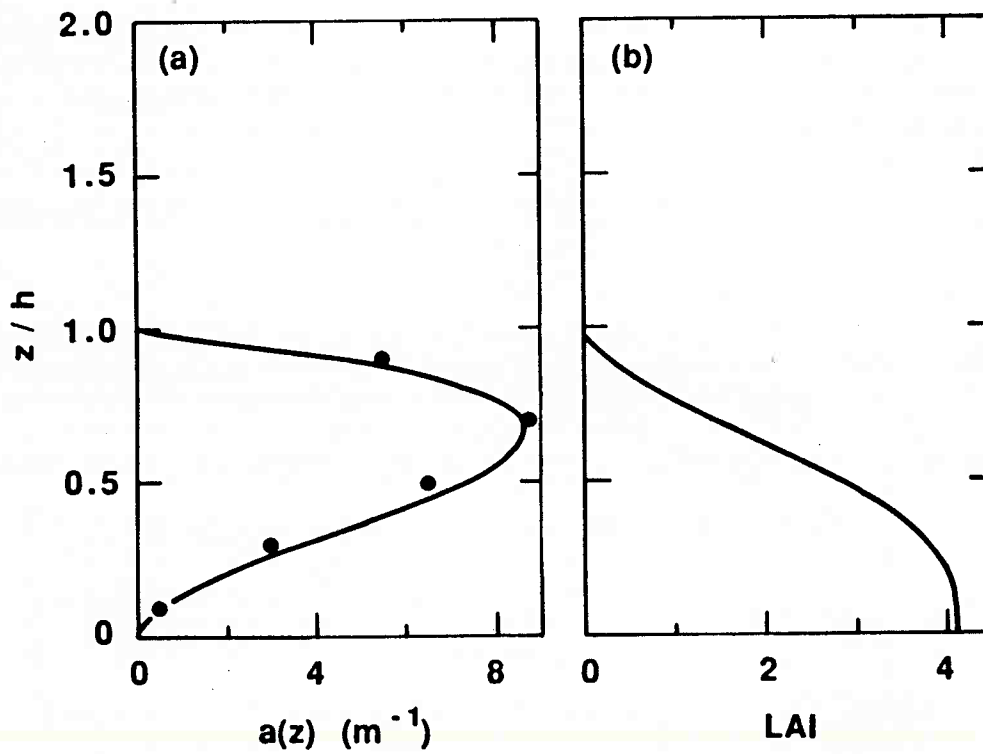
19

Fig. 3.2

Vertical profile of lead area density (a(z)) and cumulative leaf area index of soybeans growing near Mead, NE, August 4, 1979.

3.6 Measurement of Meteorological Variables and Water Vapor Concentration and Flux Density Above and Within a Soybean Canopy

Net radiation flux density was measured at an altitude of 1.85 m above the surface with a Swissteco net radiometer. The net radiation profiles inside the canopy were measured with an array of strip radiometers that were built in-house. Net radiation extinction coefficient was obtained by a best fit method, using radiation data from several days. The net radiation attenuation coefficient (Γ) was 0.55; the computed net radiation profile is shown in Fig. 3.3a. Soil heat flux was not measured at this time. It was parameterized using a relationship between measurements of G and R_n made at other times during the study. The vapor flux divergence profile is shown in Fig. 3.3b.

Canopy water vapor flux densities were inferred from micrometeorological measurements using the K-theory, gradient method. Eddy exchange coefficients (K) were calculated using the energy balance method. Table 3.2 lists the radiation and flux data for the time period of this study. The integrated source density was computed to be 0.215 g m^{-2} s^{-1}. This value was 10% less than the measured value of 0.240 g m^{-2} s^{-1}. The ratio between actual evaporation and potential evaporation (E/E_{pot}) was 1.47, which was only 13% greater than the value for the Priestly-Taylor coefficient, 1.3. The assumption of estimating the evaporative source term via the Priestly-Taylor Equation (as a function of available net radiation) is valid for our purpose of testing the models since preliminary tests show that these two different parameter values had little influence on the estimate of water vapor concentrations.

Table 3.2 Energy flux densities

Parameter	symbol	value
Net radiation	R_n	523 W/m^2
Soil heat flux coefficient	α_s	0.5
Soil heat flux	G	25.2 W/m^2
Latent heat flux	LE	583 W/m^2
Water vapor flux	E	0.238 g/m^{2}s
Sens. heat flux	H	-40.6 W/m^2

The horizontal wind speed profile above the canopy was measured with sensitive cup anemometers. Wind profile measurements were used to determine stability and canopy aerodynamic parameters. The Monin-Obukhov stability parameter z/L was 0.006, suggesting near-neutral stability; L being the Monin-Obukhov length scale. Table 3.3 lists the horizontal wind speed data. Wind speed profiles were measured between and within rows inside the canopy. Omni-directional, heated thermistor anemometers were used (see Baldocchi, 1982). These data were averaged to obtain one mean profile.

Table 3.3 Horizontal wind speed parameters.

Parameter	symbol	value
Friction velocity	u*	0.61 m s^{-1}
Wind speed at 2.0 m	u(2)	3.93 m s^{-1}
Wind speed at z=h	u(h)	1.90 m^{-1}
wind attenuation coef.	γ	1.935

Temperature and water vapor pressure were measured inside and above the canopy up to a height of 3 m. A reversing psychrometer was used to measure temperature and humidity above the canopy (Rosenberg and Brown, 1974). Wind aspirated psychrometers were used to measure within canopy temperatures and humidities (Stitger and Welgraven, 1976). Psychrometers should be exposed to air speeds exceeding 4 m s^{-1} to avoid convection errors. Wind speeds inside a plant canopy were much less than this figure, so we developed empirical relationships in a wind tunnel between the mini psychrometer output and wind speed (Fig. 3.4). We used these relationships to correct the within canopy psychrometers measurements to aspiration rates of 4.0 m s$^{-1.}$ Table 3.4 gives the normalized humidity data measured above and within the canopy. The water vapor concentration is normalized by u*/Q. The reference height for determining the relative water vapor concentration was chosen to be 3 m.

Table 3.4 Measured temperature and humidity data for August 4,1979. Hourly averaged humidity data, taken between 11 am and 2 pm, is averaged to produce the final values.

z (m)	z/h	e (mb)	e$_s$ (mb)	ρ_v (g m^{-3})[**]	ρ_v-$\rho_{v,r}$[**]
0.10	0.12	30.28	53.17	18.82	3.609
0.30	0.35	29.80	54.06	18.87	3.722
0.50	0.59	29.88	55.82	19.41	5.127
0.70	0.82	28.80	55.21	19.38	5.010
0.90	1.06	26.70	54.18	18.80	3.473
1.00	1.18	26.46	51.91	18.68	3.136
1.25	1.47	26.13	51.86	18.45	2.557
1.50	1.76	25.82	51.95	18.23	1.996
2.00	2.35	25.32	52.22	17.87	1.084
2.50	2.94	24.91	52.19	17.58	0.356
3.00	3.53	24.70	52.31	17.43	0.00

[*]: $\rho_{v,r}$ = reference concentration, at z=3 m.
[**]: normalized by u*/Q

22

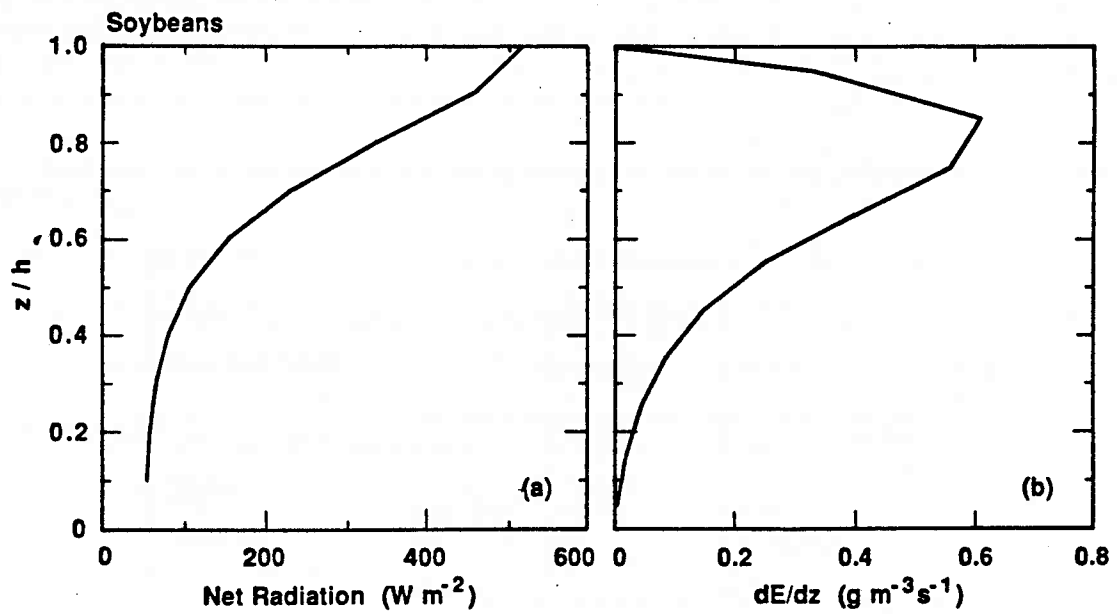**Fig. 3.3**

Computed profile of net radiation and the water vapor flux divergence in a soybean canopy near Mead, NE, August 4, 1979.

ATDL-M 89/1164

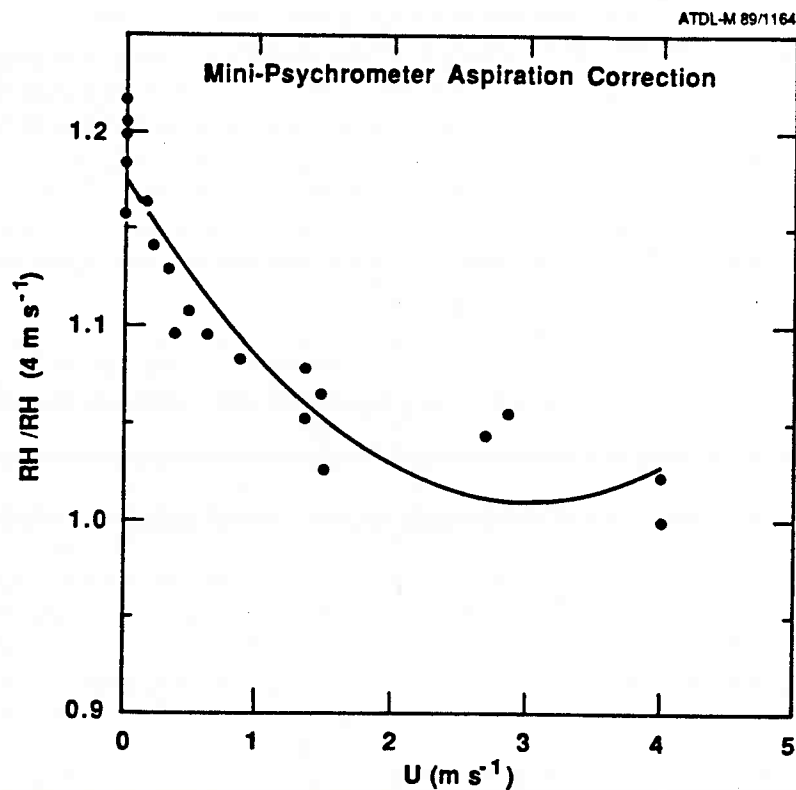**Mini-Psychrometer Aspiration Correction**

Fig. 3.4

Correction coefficient for the Stitger and Welgraven (1976) minipsychrometers. These were developed empirically in a wind tunnel. Relative humidities are corrected to an aspiration velocity of 4 m s^{-1}.

4. RESULTS OF MODEL SIMULATIONS

In this chapter we test and discuss the random walk models derived from the algorithms of Legg and Raupach (1982), Wilson et al. (1983) and Thompson (1984). We will also compare the Lagrangian models against the Eulerian model of Meyers and Paw U (1987).

4.1 Parameterization Tests

Before we can test the random walk models we address several issues. Of foremost importance, we must choose the proper time step for parcel motion and we need to know how many fluid parcels to release.

Trajectories of fluid parcels were computed with a time step (Δt) equal to 0.025 T_L(h). This choice is a based on sensitivity tests of the model. An equilibrium flux profile is commonly observed for mass, energy and momentum transfer over a surface in a fully-developed boundary layer. Fig. 4.1 shows that this is not reached until Δt is equal to or smaller than 0.05 T_L(h). The concentration profile, on the other hand, is less affected by the time step.

Table 4.1 Input parameters for the simulation of water vapor concentration and vertical flux profile for August 4, 1979.

parameter	symbol	value
grid cell height	Δz	0.1 h
number of measurement layers	n_{lay}	40
time step length	Δt	0.025T_L

The number of particles is also crucial in generating numerically stable profiles with a random walk model. An optimal number of released parcels must be determined to economize on computer time, yet reduce the statistical noise associated with an inadequate number of particles. We found that 5000 parcels is sufficient to achieve a stable and repeatable concentration and flux profile (Fig. 4.2). Smaller numbers of released parcels results in 'noisy' profiles and run-to-run variability.

The ultimate test of a random-walk model is whether or not it attains mass conservation. For the one-dimensional case, the canopy source—the amount of material released per unit area—must equal the integral of concentration profile. In other words, all the material released must be accounted for in the atmosphere:

$$QT - \int_0^{\infty} c(z)dz \qquad (59)$$

where T is travel time. To test whether the conservation of mass was achieved, the model domain was extended to 8 times canopy height. We found, for a 5 second travel time, that Q*T equalled 1.07 g m^{-2} and the integrated concentration profile equalled 1.09 g m2m, a 2% difference, thereby confirming conservation of mass.

4.2 Model Evaluation

a: Legg and Raupach (1982)

The evolution of the normalized concentration and flux profiles that were computed with the algorithm of Legg and Raupach (1982) (Eq. 37) are shown in Figs. 4.3a and 4.3b, respectively. Profile shapes evolve until equilibrium is reached after a 100 s travel time. Normalized concentrations decrease with height above the canopy. In the upper third of the canopy one observes that the water vapor profile has a prominent 'nose'. This bulge occurs near the level where the source strength is maximal (Fig. 3.3). Below this level humidities decrease. The shape of the within canopy concentration profile is significantly influenced by near-field sources (Raupach, 1987). It is of interest to note that the shape of the water vapor profile inside the canopy differs from the hypothetical profile that is commonly shown in textbooks (Monteith, 1973). It is important to recognize that many water vapor profiles reported in the literature may be based on data derived from inadequately aspirated psychrometers.

Flux profiles vary with height above the canopy until an equilibrium and constant profile is achieved. As with the concentration field, it takes a travel time of 100 s to reach equilibrium. Inside the canopy, the evolution of the flux profile is quite complex. At small travel times (< 10s) material is transferred both upward and downward from the foliage, due to the strong influence of near-field sources, and upward from the soil. Only after long travel times (T > 50 s) does the flux profile exhibit upward transfer at all levels in the canopy.

Comparison of Figs. 4.3a and 4.3b demonstrates the theoretical occurrence of counter-gradient transport of water vapor in a soybean canopy. These data are the first to note this phenomenon for water vapor since most other results have been based on inadequately aspirated psychrometers. Counter-gradient transfer has been previously shown to occur theoretically and experimentally in plant canopies for momentum, heat, and CO_2 (Wilson and Shaw, 1977; Denmead and Bradley, 1987; Baldocchi and Meyers, 1988a). Raupach (1987) explains counter-gradient transfer in the following terms:

'At any point of observation, scalar from nearby elementary sources is dispersing in a near-field regime...which causes its contribution to the overall gradient to be greater than its contribution to the overall flux density. Just below a fairly localized and intense source in the canopy, the near-field gradient contribution is large and positive; when this is combined with the upward flux of scalar (as) required by conservation of scalar mass, a counter-gradient flux is obtained.'

Model computations are compared against field measurements in Fig 4.4. Model results mimic the same shape of the measured and normalized water vapor concentration profile. Modelled values overestimate concentrations measured above the canopy by less than 10%, except at the canopy/atmosphere interface where the difference is about 50%. Within the canopy, simulated concentrations agree within one standard error, with most of the field measurements.
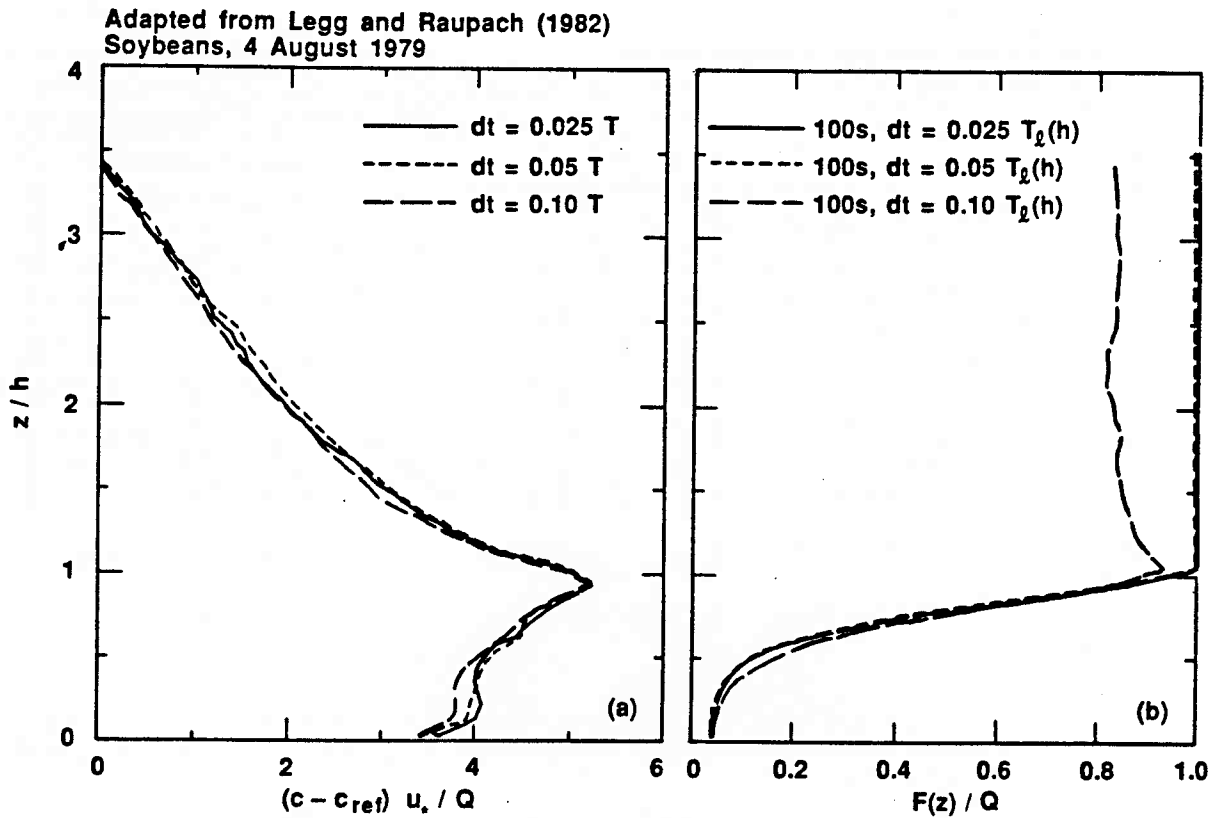
26

Fig. 4.1

Sensitivity of computations of normalized water vapor concentration and fluxes to time steps duration. These tests are based on the model adapted from the formulation of Legg and Raupach (1982).

27

Adapted from Legg and Raupach (1982)
Soybeans, 4 August 1979

(a)

n = 500
n = 1000
n = 5000
n = 10000

z / h

(c − c_ref) u_* / Q

(b)

n = 500, T = 100s
n = 1000, T = 100s
n = 2500, T = 100s
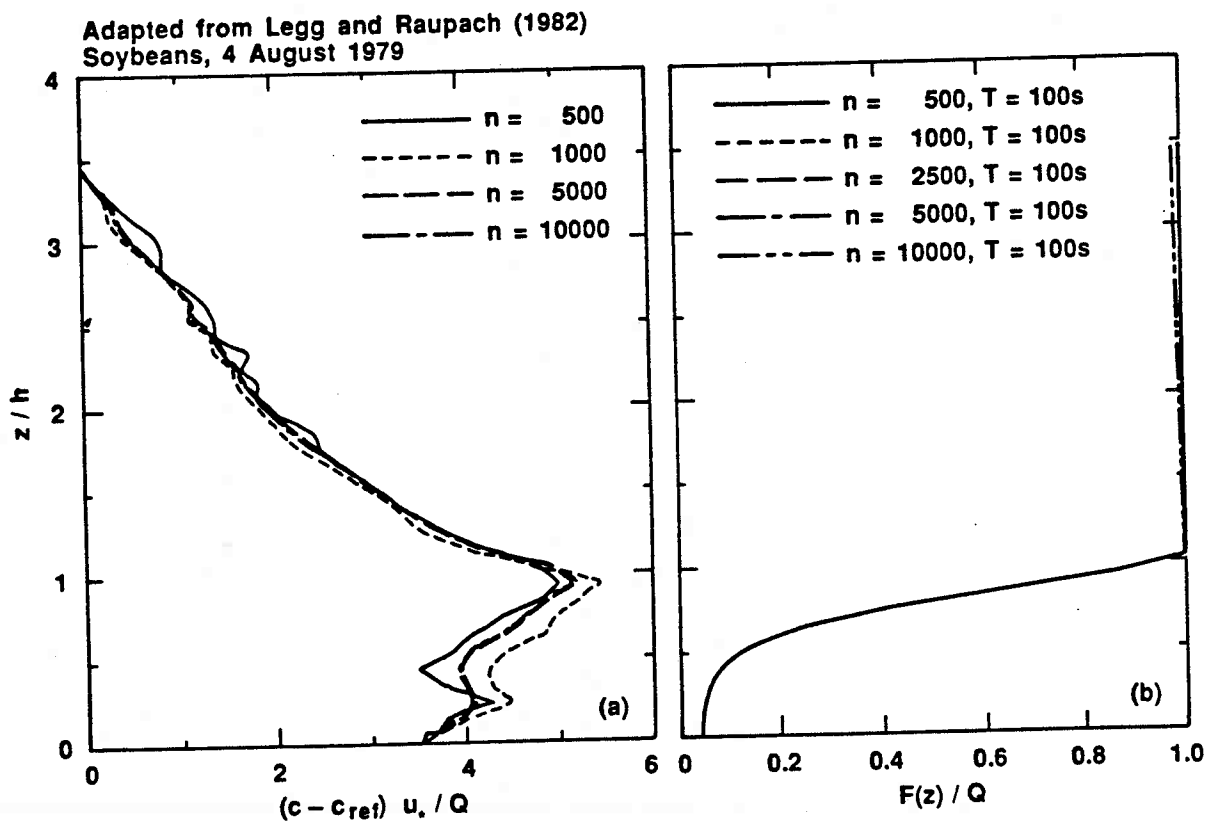n = 5000, T = 100s
n = 10000, T = 100s

F(z) / Q

Fig. 4.2

Sensitivity of computations of normalized water vapor concentration and fluxes to the number of released fluid parcels. These tests are based on the model adapted from the formulation of Legg and Raupach (1982).
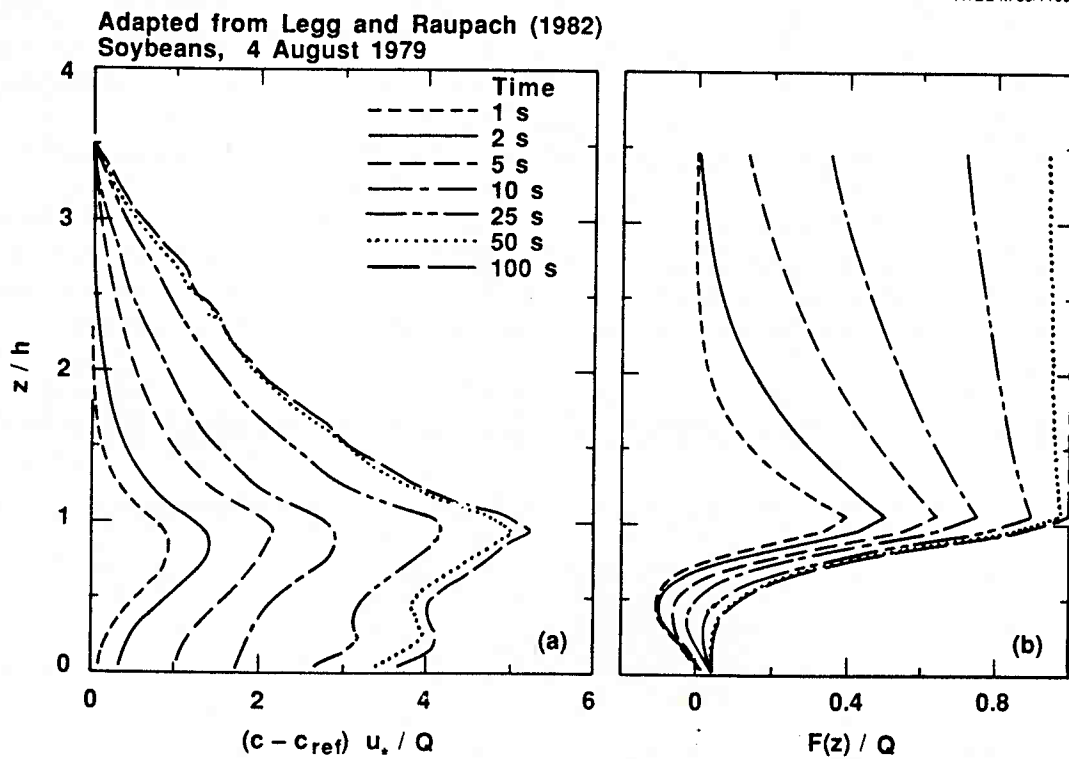
28

Fig. 4.3

The progression in normalized concentration (a) and flux (b) profiles with increasing travel time. Computations are based on the model derived from the formulations of Legg and Raupach (1982).
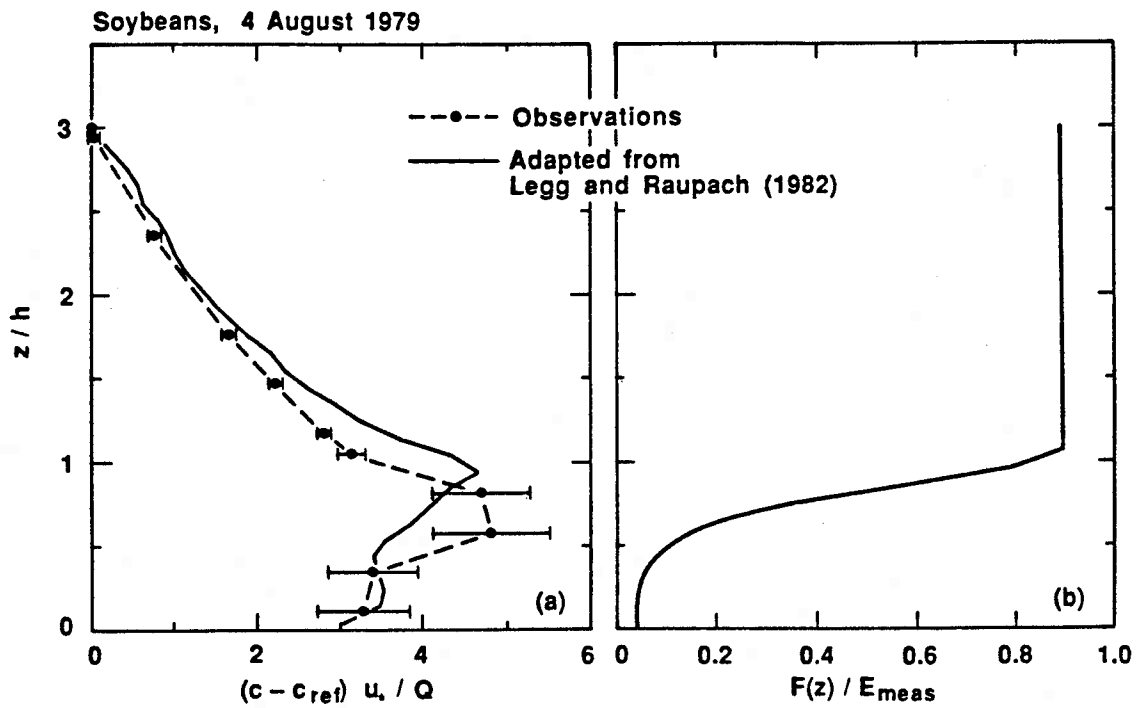
29

Soybeans, 4 August 1979

Fig. 4.4

Comparison of water vapor concentration and flux computations based on the model derived from the formulations of Legg and Raupach (1982) against measurements made in a soybean canopy.

The computed canopy water vapor flux underestimates the actual flux measurement by about 10%. Better agreement may have occurred had we used a more detailed and accurate parameterization of the source strength. This can be done by basing the source strength on the leaf energy balance; this will be the objective of our future studies. We were unable to compare flux estimates computed inside the canopy with measurements.

b: Wilson et al. (1983)

The evolution of the concentration and flux profiles computed with the algorithm of Wilson et al. (1983) (Eq. 39), are shown in Figs. 4.5a and 4.5b, respectively. The normalized concentrations decrease with height above the canopy. Inside the canopy, a nose in the concentration profile is observed only for small travel times (T < 10 s). Equilibrium concentration profiles are reached after a travel time of 100 s. Their shape is relatively uniform in the canopy, except near the soil where they decrease. The evolution of the flux profile is similar to that described for the Legg and Raupach (1982) algorithm.

Model computations are tested against measurements of water vapor concentrations and fluxes in Fig. 4.6a and 4.6b. Computations of water vapor concentration perfectly mimic measurements made above the canopy. On the other hand, model computations significantly underestimate concentrations measured in the upper canopy, where the canopy source is strongest. There is no significant difference between measured and model concentrations in the lower half of the canopy. This model also underestimates the canopy water vapor flux by < 10%. Again this is due to the parameterization scheme for the canopy source.

The upward drift velocity of the Wilson et al. (1983) (WTK") and Legg and Raupach (1982) algorithms can be compared via algebraic manipulation. They are identical if $1 \, d\sigma_w/dz$ changes slowly with height and an arising term, $(d\sigma_w/dz)^2$, is negligible. Tests by Wilson et al. (1983) show that the WTK" model gives the most physically realistic results for dispersion from a single elevated source in a corn canopy. Our tests show that this is not true in the case of a canopy with layered sources and inhomogeneous turbulence.

c: Thomson (1984)

Concentration and flux profiles computed with the algorithm of Thomson (1984) differ strongly from field measurements and values computed with the algorithm of Legg and Raupach model (Fig. 4.7). Computed concentrations exhibit an excessive depletion of water vapor inside the canopy and a constant flux layer is never achieved above the canopy after 100 s. A problem with the Thomson model stems with choosing an appropriate time step, Δt. Fig. 4.8 shows that the concentration and flux profiles are exceedingly sensitive to the choice of Δt. This is because as the time step becomes smaller the magnitude of the third moment (μ^3) increases. Consequently, the ability to accurately generate a set of random numbers with a mean of absolute zero decreases. Table 4.2 shows that an artificially high mean random numbers and mean vertical velocities occurs as the time step diminishes since Sk_μ becomes increasingly more negative. Probability distributions with large skewness values stretches the ability of any random number generation scheme to draw random numbers to its limit. The Thomson method may be theoretically sound, but it is impractical to use in non-Gaussian turbulence because its random forcing suffers from numerical instabilities.

Adapted from Wilson et al. (1983)
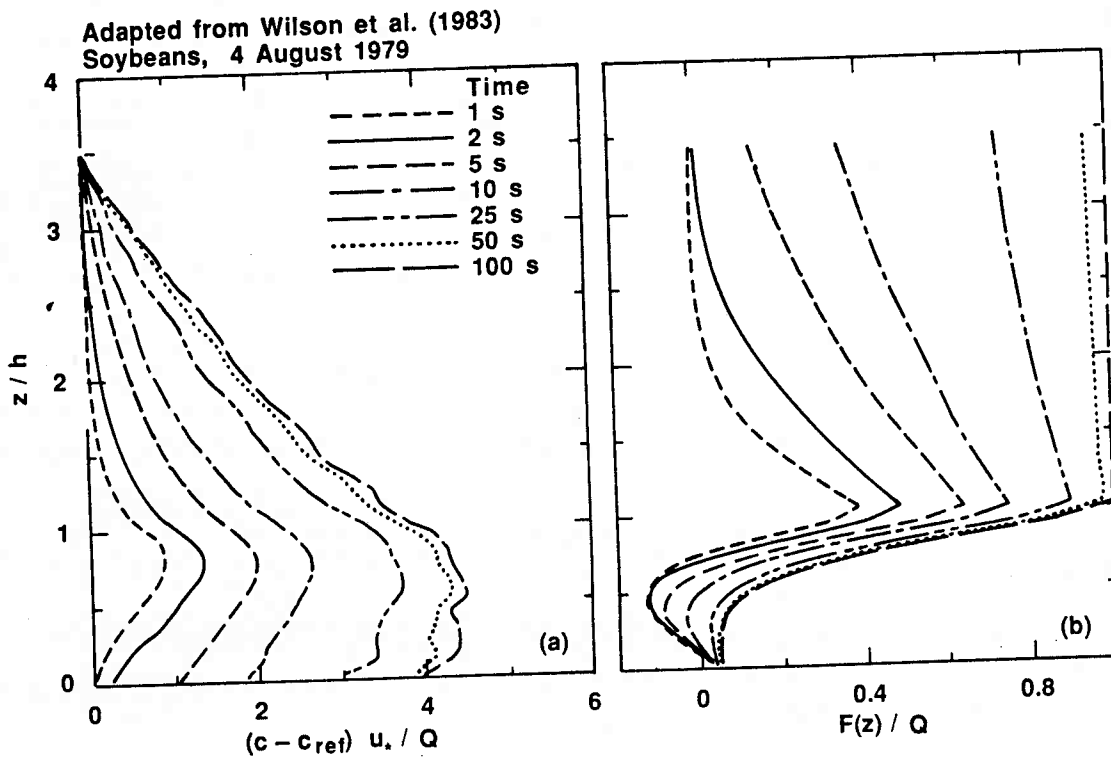**Soybeans, 4 August 1979**

Fig. 4.5

The progression in normal concentration (a) and flux (b) profiles with increasing travel time. Computations are based on the model derived from the formulations of Wilson et al. (1983).
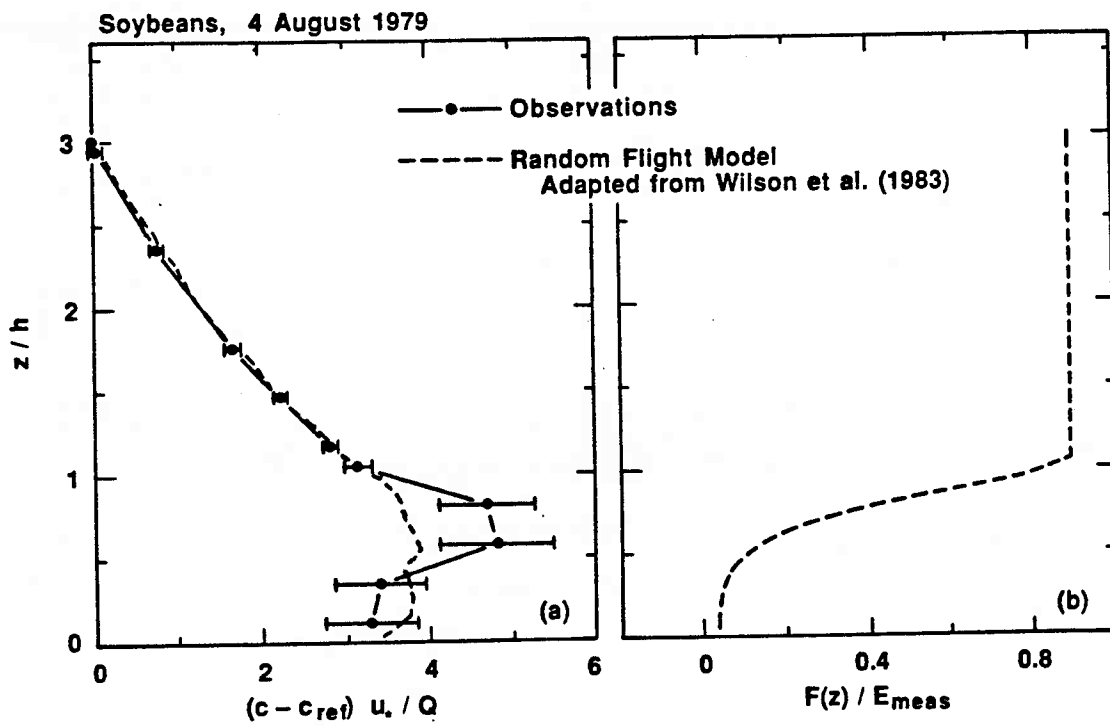
32

Fig. 4.6

Comparison of water vapor concentration and flux computations based on the model derived from the formulations of Wilson et al. (1983) against measurements made in a soybean canopy.
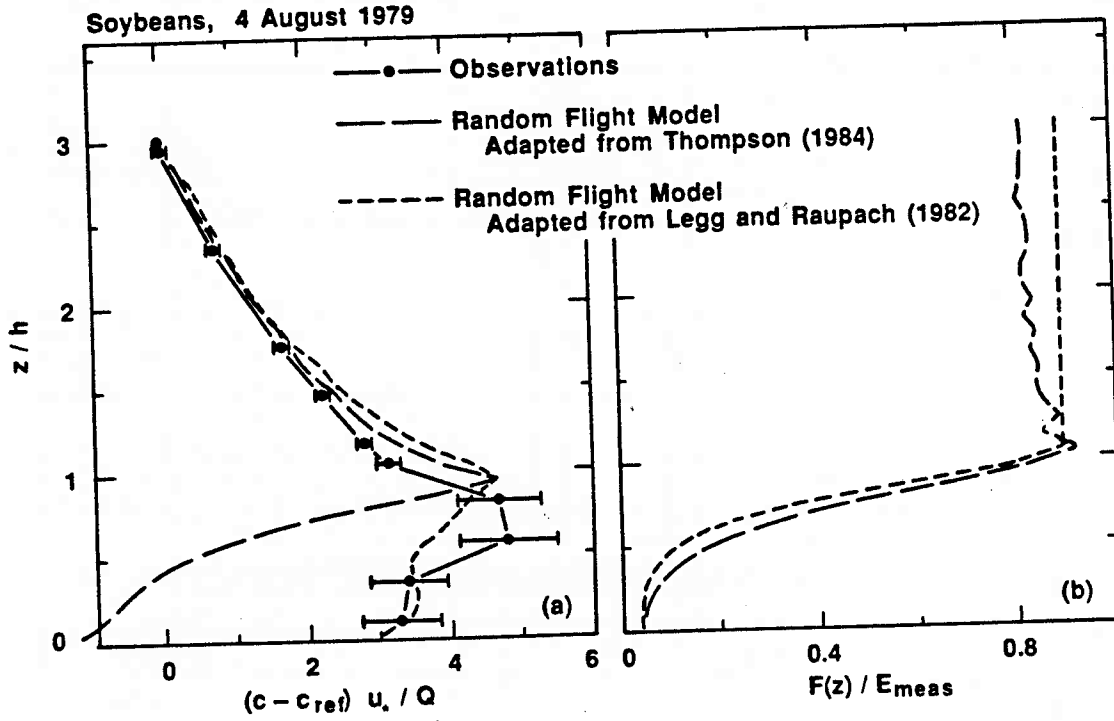
33

Fig. 4.7

Comparison of water vapor concentration and flux computations based on the model derived from the formulations of Thomson (1984) against measurements made in a soybean canopy.
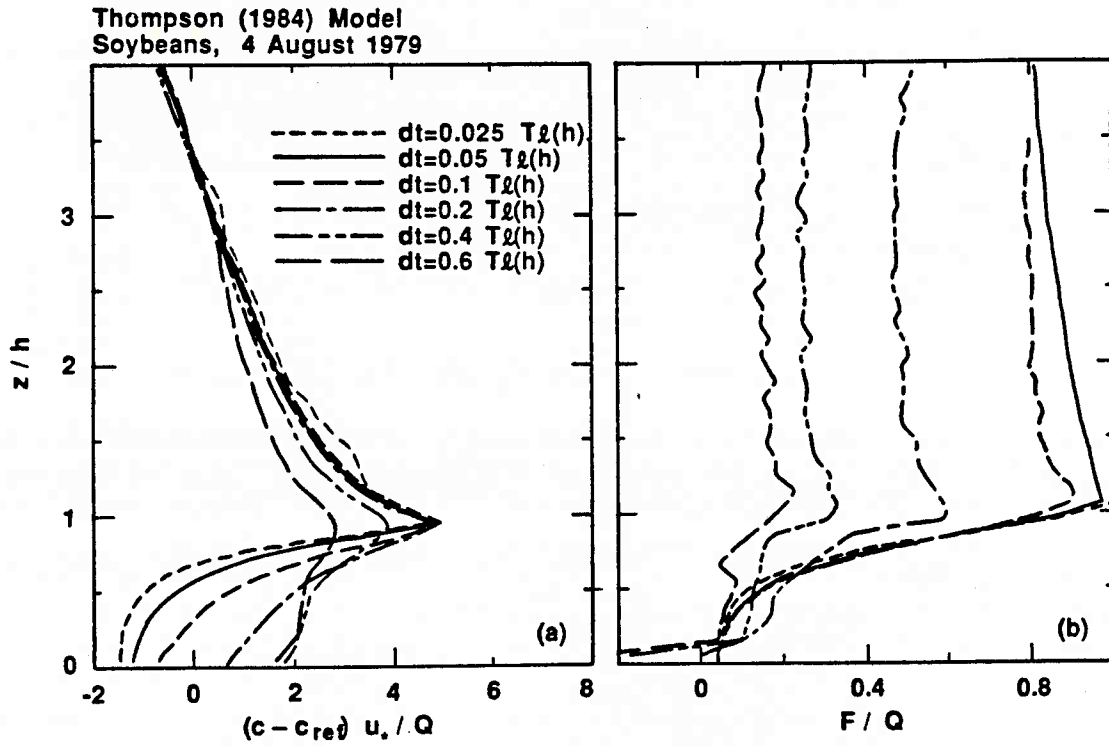
34

Fig. 4.8

The progression in normalized concentration (a) and flux (b) profiles with increasing travel time. Computations are based on the model derived from the formulations of Thomson (1984).

35

We recommend that the Thomson method be used only in homogeneous turbulence, where numerical solutions will be more stable. Thomson (1984) and Sawford (1985) have also commented on the impracticality of using Thomson's model in inhomogeneous turbulence. Yet they have not demonstrated the limitations so explicitly.

Table 4.2   The sensitivity of the Thomson model parameter

$\dfrac{dt}{T_L}$	$\overline{\mu}$	$\overline{w}$	Sk_μ
0.05	0.029	0.183	-3.003
0.10	0.029	0.168	-2.123
0.20	0.024	0.164	-1.501
0.40	0.018	0.172	-1.060
0.60	0.016	0.192	-0.870

4.3 Lagrangian Versus Eulerian Models

Fig. 4.9 shows a comparison between measured water vapor concentrations and values computed with the Lagrangian models, using random walk algorithms of Legg and Raupach and Wilson et al., and the Eulerian model of Meyers and Paw U (1987). The Eulerian model computes water vapor profiles that slightly underestimate measured values above the canopy and agree with measured values, within one standard error, in the upper half of the canopy. However, computations based on the Eulerian model significantly overestimates observed concentrations by about 50% in the lower half of the canopy. The Eulerian model also does not simulate counter-gradient transport of water vapor, as was simulated with the Lagrangian model; albeit Eulerian models are capable of simulating counter gradient transfer (Wilson and Shaw, 1977). Computations of canopy water vapor flux densities derived from the Lagrangian and Eulerian models are nearly identical, in spite of the fact that the Eulerian model treats the estimate of the water vapor source in greater detail.

The sensitivity of the Lagrangian model to turbulence statistics can be tested by using the σ_w/u^* profile computed with the Eulerian model. Fig. 4.10 shows the vertical profile of σ_w/u^* computed with the model of Meyers and Paw U (1986). These values are greater than the values based on the parameterization of Hunt and Weber (1979) and Wilson et al. (1982). Larger turbulence levels in the canopy disperse material more (Fig. 4.11). This effect reduces concentrations in the canopy, and thereby seriously underestimates measured values. Based on this comparison, it seems that the simple parameterization scheme of σ_w/u^* by Hunt and Weber (1979) and Wilson et al. (1982) is adequate for Lagrangian modelling.

Soybeans, 4 August 1979

Fig. 4.9

Comparison of water vapor concentration and flux computations based on the model derived from the formulations of Legg and Raupach (1982), Wilson et al. (1983) and Meyers and Paw U (1987) against measurements made in a soybean canopy.

37

Soybeans
Computed with Higher Order Closure Model
of Meyers and Paw U (1986)

Fig. 4.10

Vertical profile of the standard deviation of normalized vertical velocity in a soybean canopy, as computed with the Eulerian model of Meyers and Paw U (1986).
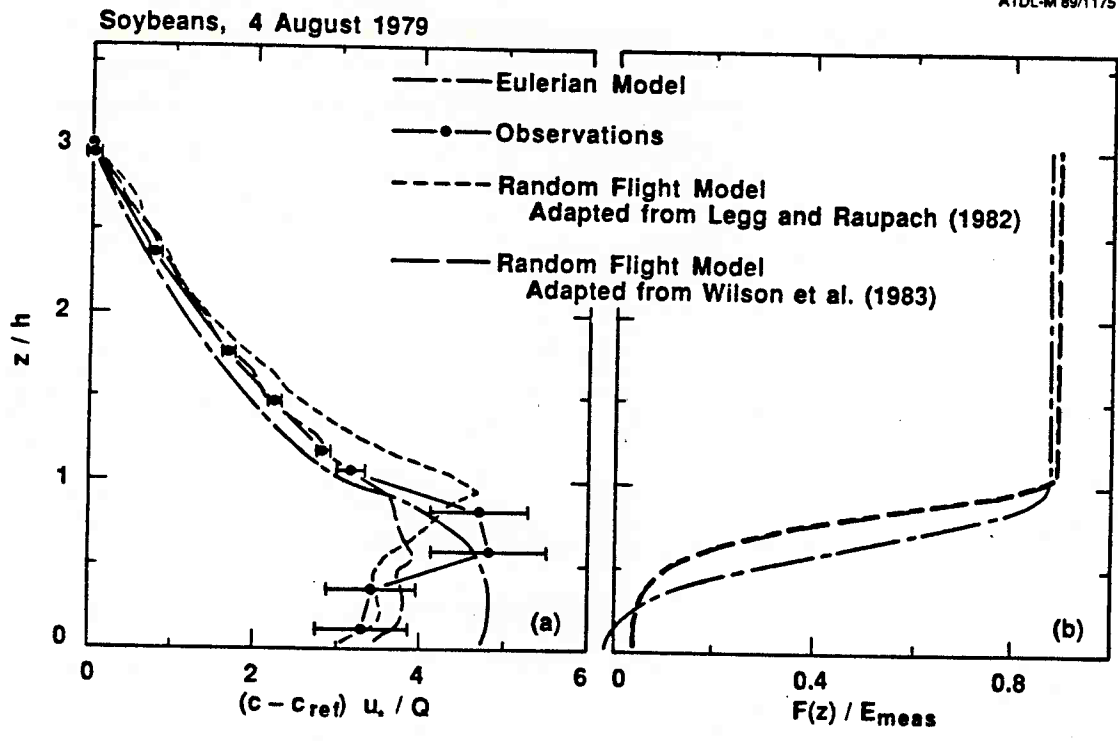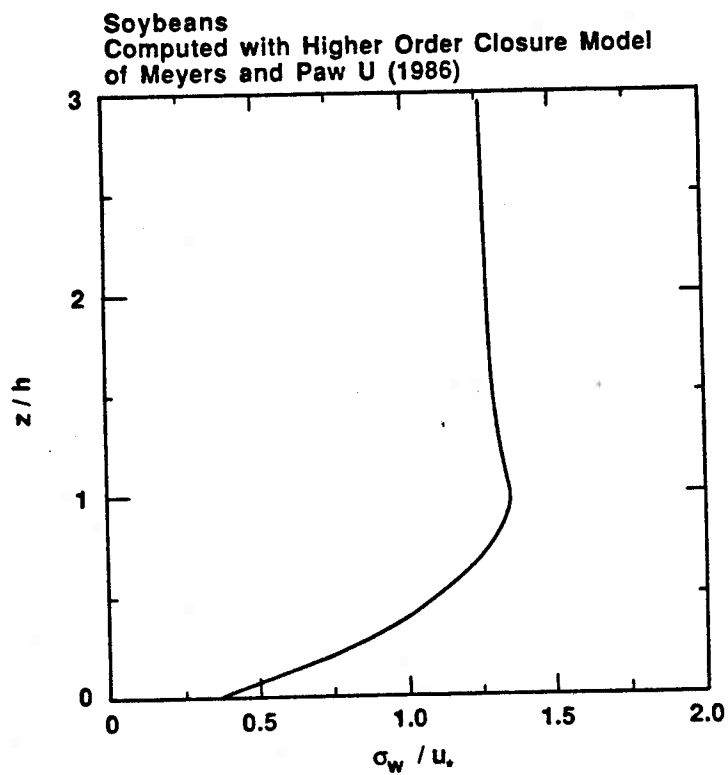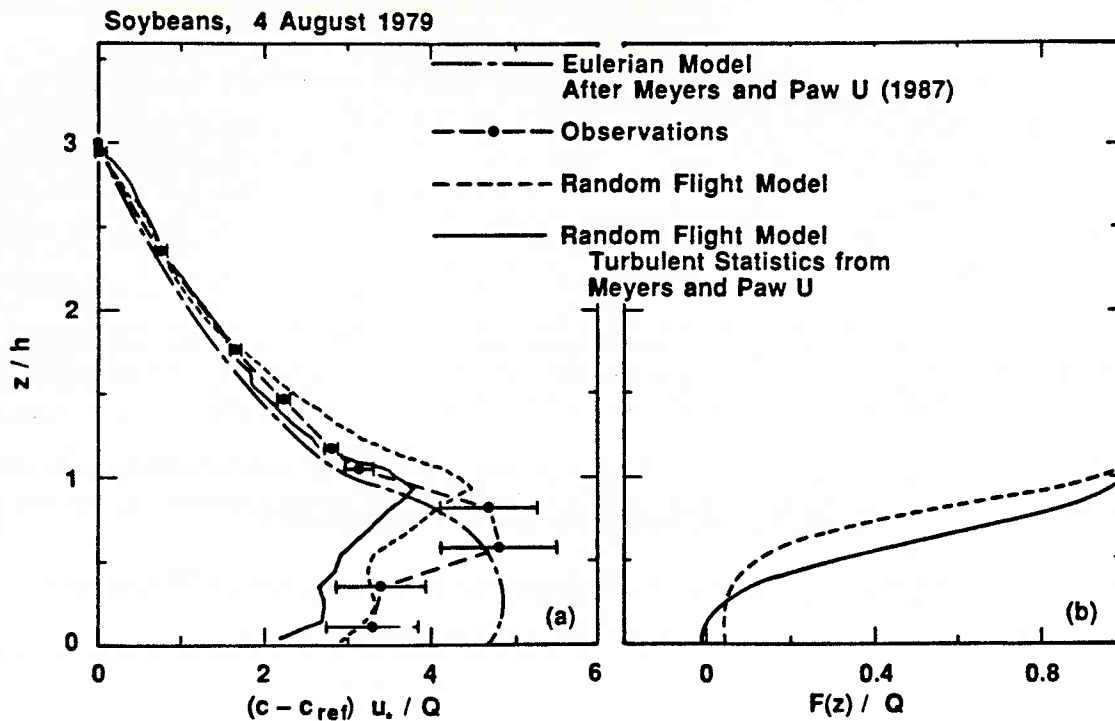
38

Fig. 4.11

Comparison of water vapor concentration and flux computations based on the model derived from the formulations of Legg and Raupach (1982) using the turbulence parameterization based on Hunt and Weber (1979) and Meyers and Paw U (1987). These are compared against computations derived from Meyers and Paw U (1987) and against water vapor measurements made in a soybean canopy.

5. SUMMARY, CONCLUSIONS AND RECOMMENDATIONS

5.1 Summary

Three Lagrangian random walk models were developed for computing the exchange of water vapor in a soybean canopy; we used the algorithms of Legg and Raupach (1982), Wilson et al. (1983) and Thomson (1984) to compute the trajectory of fluid parcels. Sources strengths of water vapor were computed according to the net radiation flux density computed at multiple layers in the canopy. The models were tested against field measurement and were compared against computations based on an Eulerian higher order closure model (Meyers and Paw U, 1987). Sensitivity tests were performed to examine the influence of turbulence parameters and model parameters.

Computations of water vapor profiles using Lagrangian random walk models based on the theory of Legg and Raupach and Wilson et al. agree well with measured water vapor profiles. The Lagrangian model based on the theory of Thomson, on the other hand, computes water vapor profiles that severely underestimate measured values. The model based on the Legg and Raupach formulation does a better job of predicting the water vapor concentration field inside the canopy, while the model based on the algorithm of Wilson et al. yields more accurate computations of the concentration field above the canopy. Formulations based on the models of Legg and Raupach and Wilson et al. mimic the shape of the water vapor profile inside the canopy more realistically than do computations based on the Eulerian model of Meyers and Paw U (1987). This is because Lagrangian models explicitly account for near-field diffusion while Eulerian models do not.

The Thomson model, though theoretically rigorous, suffers from numerical impracticalities; imposing smaller time steps yields a more negatively skewed third order moment for the random forcing term, which causes the accuracy of the computed random number table to decrease. The Thomson model is also incapable of computing a constant flux layer after 100 s travel times, unlike the other models.

5.2 Conclusions

Eulerian models have been used for over two decades to model the canopy microenvironment (see Raupach and Thom, 1981). Development of Lagrangian models is more recent, but has progressed rapidly in the current decade. Lagrangian models have been promoted as an alternative method to circumvent the limitations and uncertainties associated in closing the system of equations in Eulerian models (Raupach, 1987, 1988, 1989). In actuality, both Eulerian and Lagrangian models for turbulence transfer in plant canopies suffer from particular closure problems. Eulerian models use parameterization schemes to close a set of rate equations of first and higher order moments. Lagrangian models need a specified turbulence field, which can only be known from field measurements or model parameterization, to attain 'closure'. Furthermore, the Lagrangian models are based on Langevin's Equation, which has no theoretical basis. Consequently, both classes of models must be tested in the field environment.

The most fundamental weakness of Eulerian models is an inability to capture the influence of near-field sources on the concentration field. Ultimately, the model must be closed at higher orders with an assumption of down-gradient diffusion, which uses an effective eddy exchange coefficient that is valid only at the limit of far-field diffusion. In actuality, turbulence diffusion from

nearby sources is strongly dependent on time of release (Deardorff, 1978). Deardorff's analysis suggests that closure errors cannot be minimized if done at higher moments.

The relative strength of Lagrangian models is their capability to account for the contributions of both near-and-far-field sources or sinks on concentration fields and fluxes. Although the Lagrangian models require a specified turbulence field, this requirement is not overly restricting. Raupach (1988) shows that canopy height and u^* are the dominant length and velocity scales. Scaling with these variables causes measurements from disparate canopies (heights varying by a factor of 400) and turbulence regimes (u^* values varying by a factor of 10) to collapse onto a somewhat general curve.

Raupach has demonstrated that analytical modelling schemes, which require assumptions of homogeneous turbulence, succeed in simulating concentration measurements in wind tunnels from a single elevated source. Measurements of turbulence in plant canopies show that the turbulence field is distinctly inhomogeneous (Wilson et al., 1982; Baldocchi, 1988a) and that multiple sources occur. This is the basis of our decision to use a more complex and a computationally demanding numerical random walk model instead. In fact, if there is any one restricting trade-off in using a Lagrangian model over a Eulerian model, it would be one associated with the economy of computer time. While the random-walk Lagrangian model may be conceptually simpler, it requires much more computer time; for example: 3.5 hrs are needed on a Compaq 386/20 to compute steady state profiles with 100 s travel times, while the Eulerian model of Meyers and Paw U (1986) only requires several minutes of computer time.

5.3 Recommendations: Other Applications of the Model

Further improvements in the Lagrangian model are obvious and will be the focus of future activity. Further development and testing of simple analytical Lagrangian models is required. We must also consider cases where the source, or sink, is a function of the local concentration field. Some effort is being made by Mike Raupach and we hope to extend this work.

The model presented here can, in principal, also be modified and applied for the describing of the transfer and dispersion of components other than water vapor (CO_2, pollutants, pollen, spore) inside plant canopies. For CO_2 exchange it is necessary to consider the foliage as a sink, while the soil acts as a source. The vertical sink strength distribution for CO_2 inside a canopy depends on its photosynthetic activity. This requires computing vertical variations in light (PAR), leaf temperature, leaf-air vapor pressure differences, stomatal and boundary layer resistances, and CO_2 concentration, among other factors. The canopy Lagrangian model also has great potential for computing the relative roles of turbulent exchange and chemical reactivity in dealing with the uptake, emission, and transformation of chemically active species and their precursors. Finally, Lagrangian models can be used in two dimensional studies of the role of source/sink spatial heterogeneity on sub-grid parameterizations of larger scale models.

ACKNOWLEDGEMENTS

REFERENCES

Aylor, D.E. and F.J. Ferrandino. 1989. Dispersion of spores released from an elevated line source within a wheat canopy. *Boundary-Layer Meteorol.* 46:251-273.

Baldocchi, D.D. and B.A. Hutchison. 1987. Turbulence in an almond orchard: vertical variations in turbulent statistics. *Boundary-Layer Meteorol.* 40:127-146.

Baldocchi, D.D. and T.P. Meyers. 1988a. Turbulence Structure in a Deciduous Forest. *Boundary Layer Meteorol.* 43:345-364.

Baldocchi, D.D. and T.P. Meyers. 1988b. The effects of extreme turbulent events on the estimation of aerodynamic variables in a deciduous forest canopy; to be published in *Agricultural and Forest Meteorology.*

Baldocchi, D.D. 1982. Mass and energy exchanges of soybeans: microclimate-plant architectural interactions; Center for Agricultural Meteorology and Climatology/ Institute of Agriculture and Natural Resources/ University of Nebraska-Lincoln.

Brutsaert, W.H. 1982. *Evaporation into the atmosphere*; D. Reidel Publishing Company, Dordrecht, Boston, London.

Choudhury, B.J., Idso, S.B. and Reginato, R.J. 1987. Analysis of an empirical model for soil heat under a growing wheat crop for estimating evaporation by infrared-temperature based energy balance equation. *Agriculture Forest Meteorology.* 39: 283-297.

Cionco, R.M. 1972. A wind-profile index for canopy flow. *Boundary-Layer Meteorol.* 3:255-263.

Corrsin, S. 1974. Limitations of gradient transport models in random walks and in turbulence. *Advances in Geophysics.* 18A:25-60.

Deardorff, J.W. 1978. Closure of second- and third-moment rate equations for diffusion in homogeneous turbulence. *Physics of Fluids.* 21:525-530.

Denmead, O.T. 1964. Evaporation sources and apparent diffusivities in a forest canopy; *J. Appl. Met.* 3:383-384.

Denmead, O.T. and E.F. Bradley. 1985. Flux-gradient relationships in a forest canopy; In *Forest-Atmosphere Interactions*, Ed. by B.A. Hutchison and B.B. Hicks. Reidel Publ. Co., Dordrecht, pp 421-442.

Denmead, O.T. and E.F. Bradley. 1987. On scalar transport in plant canopies. *Irrig. Sci.* 8:131-149.

Durbin, P.A. 1980. A random flight model of inhomogeneous turbulent dispersion; *Physics of Fluids* 23:2151-2153.

Finnigan, J.J. and M.R. Raupach. 1987. Transfer Processes in Plant Canopies in Relation to Stomatal Characteristics; In *Stomatal Functions*; ed. by Zeiger et al.; Stanford University Press.

Gao, W., R.H. Shaw and K.T. Paw U. 1989. Observation of organized structure in turbulent flow within and above a forest canopy. *Boundary-Layer Meteorol.* 47:349-377.

Hall, C.D. 1975. The simulation of particle motion in the atmosphere by a numerical random-walk model; *Quart. Journ. Roy. Meteorol. Soc.* 101:235-244.

Hunt, J.C.R. and A.H. Weber. 1979. A Lagrangian Statistical Analysis of Diffusion from a Ground-Level Source in a Turbulent Boundary Layer. *Quart. Journ. Roy. Meteorol. Soc.* 105:423-443.

Jarvis, P.G. and K.G. McNaughton. 1986. Stomatal Control of Transpiration: Scaling Up from Leaf to Region. *Advances in Ecological Research.* 15:1-49.

Lamb, R.G. 1980. Mathematical principles of turbulent diffusion modeling. In *Atmospheric Boundary Layer Physics*, ed. A. Longhetto. Elsevier Sci. Pub. pp 173-210.

Legg, B.J. 1983. Turbulent Dispersion from an Elevated Line Source: Markov-Chain Simulations of Concentration- and Flux-profiles. *Quart. Journ. Roy. Meteorol. Soc.* 109:645-660.

Legg, B.J. and M.R. Raupach. 1982. Markov-chain Simulation of Particle Dispersion in inhomogeneous Flows: the mean drift Velocity induced by a Gradient in Eulerian Velocity Variance. *Boundary Layer Meteorol.* 24:3-13.

Leclerc, M.Y., G.W. Thurtell, and G.E. Kidd. 1988. Measurements and Langevin Simulations of Mean Tracer Concentration Fields Downwind from a Circular Line Source inside an Alfalfa Canopy. *Boundary-Layer Meteorol.* 43:287-308.

Meyers, T.P and K.T. Paw U. 1986. Testing of a higher-order closure model for modeling airflow within and above plant canopies. *Boundary-Layer Meteorol.* 37:297-311.

Meyers, T.P and K.T. Paw U. 1987. Modelling the plant canopy micrometeorology with higher-order closure principles. *Agricultural and Forest Meteorology.* 41:143-163.

Monteith, J.L. 1973. *Principles of Environmental Physics.* E. Arnold. London. 235 pp.

Priestly, C.H.B. and R.J. Taylor. 1972. On the assessment of surface heat flux and evaporation using large-scale parameters. *Month. Weather Rev.* 100:81-92.

Raupach, M.R. 1987. A Lagrangian analysis of scalar transfer in vegetation canopies. *Quart Journ. Roy. Meteorol. Soc.* 113:107-120.

Raupach, M.R. 1988. Canopy Transport Processes; In *Flow and transport in the natural environment*; ed. by W.L. Steffen and O.T. Denmead; Springer-Verlag, Berlin.

Raupach, M.R. 1989. A practical Lagrangian method for relating scalar concentrations to source distributions in vegetation canopies. *Quart. Journ. Roy. Meteorol. Soc.* 115:609-632.

Raupach, M.R., P.A. Coppin, and B.J. Legg. 1986. Experiments on scalar dispersion within a model plant canopy; Part I: the turbulence structure. *Boundary-Layer Meteorol.* 35:21-52.

Raupach, M.R. and A.S. Thom. 1981. Turbulence in and above plant Canopies. *Ann. Rev. Fluid Mech.* 13:97-129.

Reid, J.D. 1979. Markov Chain Simulations of Vertical Dispersion in the neutral Surface Layer for Surface and Elevated Releases. *Boundary-Layer Meteorol.* 16:3-22.

Rosenberg, N.J. and K.W. Brown. 1974. Self checking psychrometer systems for gradient and profile determinations near the ground. *Agric. Meteorol.* 13:215-226.

Sawford, B.L. 1984. The Basis for, and some Limitations of the Langevin Equation in Atmospheric Relative Dispersion Modelling. *Atmosph. Env.* 18:2405-2411.

Sawford, B.L. 1985. Lagrangian statistical simulation of concentration mean and fluctuation fields. *J. Clim. and Appl. Meteorol.* 24:1152-1166.

Spanier, J. and E.M. Gelbard. 1969. *Monte Carlo Principles and Neutron Transport Problems.* Addison-Wesley Pub. Co. Reading, MA. 234 pp.

Stitger, C.J. and A.D. Welgraven. 1976. An improved radiation protected differential psychrometer for crop environment. *Arch. Met. Geophs. Biokl.* 24B:177-181.

Taylor, G.I. 1921. Diffusion by continuous movements. *Proc. Lond. Math Soc.* 2,20,196-212.

Tennekes, H. and J.L. Lumley. 1972. *A first course in turbulence*; MIT-press, Cambridge, Massachusetts.

Thomson, D.J. 1984. Random walk modelling of diffusion in inhomogeneous turbulence. *Quart. Journ. Roy. Meteorol. Soc.* 110:1107-1120.

von Mises, R. 1964. *Mathematical Theory of Probability and Statistics.* Academic Press. New York. 694 pp.

Walklate, P.J. 1987. A random-walk model for dispersion of heavy particles in turbulent air flow. *Boundary Layer Meteorol.* 39:175-190.

Wilson, J.D. 1989. Turbulent transport within the plant canopy. In *Estimation of Areal Evapotranspiration.* (eds) T.A. Black, D.L. Spittlehouse, M. Novak and D.T. Price. IAHS Press, Wallingford, UK pp 43-80.

Wilson, J.D., G.W. Thurtell, and G.E. Kidd. 1981a. Numerical simulation of particle trajectories in inhomogeneous turbulence, I: systems with constant turbulent velocity scale. *Boundary-Layer Meteorol.* 21:295-313.

Wilson, J.D., G.W. Thurtell, and G.E. Kidd. 1981b. Numerical simulation of particle trajectories in inhomogeneous turbulence, II: systems with variable turbulent velocity scale. *Boundary-Layer Meteorol.* 21:423-441.

Wilson, J.D., G.W. Thurtell, and G.E. Kidd. 1981c. Numerical simulation of particle trajectories in inhomogeneous turbulence, III: comparison of predictions with experimental data for the atmospheric surface layer. *Boundary-Layer Meteorol.* 21:443-463.

Wilson, J.D., D.P. Ward, G.W. Thurtell, and G.E Kidd. 1982. Statistics of atmospheric turbulence within and above a corn canopy. *Boundary-Layer Meteorol.* 24:495-519.

Wilson, J.D., B.J. Legg, and D.J. Thomson. 1983. Calculation of particle trajectories in the presence of a gradient in turbulent-velocity variance. *Boundary-Layer Meteorol.* 27:163-169.

Wilson, N.R. and R.H. Shaw. 1977. A Higher Order Closure Model for Canopy Flow. *Journal of Applied Meteorology* 16:1197-1205.